AIAA JOURNAL
Vol. 47, No. 3, March 2009

Geometrically Nonlinear First-Order Shear Deformation Theory for General Anisotropic Shells

Alberto Pirrera* and Paul M. Weaver†
University of Bristol, Bristol, England BS8 1TR, United Kingdom

DOI: 10.2514/1.41538

A generalized first-order shear deformation theory for anisotropic multilayered shells is presented. It includes the effects of geometrically nonlinear deformations and general initial curvature. The field equations are expressed in orthogonal conjugate curvilinear coordinates in the shell's middle surface. Hence, this formulation is particularly suitable for the analysis of monocoque structures formed using the increasingly exploited fiber-placement manufacturing techniques. A novel expression for the stiffness matrix is presented in which the relationship between the shell shape and the stiffness coefficients is highlighted. It is also shown that the stiffnesses herein obtained may lead to significantly different deformation fields from those based upon flat-plate expressions.

Nomenclature

A_1, A_2	=	Lamé coefficients
A_{ij}, B_{ij}, D_{ij}	=	stiffness matrix coefficients
A_{ij}, B_{ij}, Δ_{ij}, Γ_{ij}	=	stiffness matrix coefficients
a_1, a_2	=	scale factors
E, F, G	=	surface metric tensor elements
E_{ij}, Z_{ij}, H_{ij}	=	stiffness matrix coefficients
e_{11}, e_{22}	=	linear elongation of those line elements having (before deformation) directions coincident with the coordinate directions
e_{12}, e_{13}, e_{23}	=	linear shear deformations between those line elements having (before deformation) directions coincident with the coordinate directions
I_0, I_1, I_2	=	mass inertias
K_s	=	shear correction factor
N_{ij}, M_{ij}, Q_{ij}	=	stress resultants per unit length
$\bar{Q}_{ij}$	=	transformed stiffnesses referred to the laminate coordinate directions
$\mathbf{R}$	=	position vector of an arbitrary point
R_1, R_2	=	normal radii of curvature of the middle surface
$\mathbf{r}$	=	position vector of a point on the middle surface
u, v, w	=	displacements
u_0, v_0, w_0	=	displacements of the middle surface of the shell
δK	=	virtual variation of the kinematic energy
δU	=	virtual variation of the strain energy
δV	=	virtual variation of the potential of the applied forces
ε_{ij}	=	nonlinear strain components
ε_{11}, ε_{22}	=	nonlinear elongation of those line elements having (before deformation) directions coincident with the coordinates directions
ε_{12}, ε_{13}, ε_{23}	=	nonlinear shear deformations (change of angles) between those line elements having (before deformation) directions coincident with the coordinate directions
ξ_1, ξ_2, ζ	=	orthogonal curvilinear coordinates
σ_i	=	stress components
ϕ_1, ϕ_2	=	rotations of a normal to reference surface
ω_1, ω_2, ω_3	=	components of the curl of the displacement field

I. Introduction

ONE of the most remarkable features of composite materials is their versatility that allows engineers to design not only a structure but also its constituent material. Partly due to their excellent specific stiffness, there is often the tendency to use them to replicate the well-known behavior of isotropic materials, thus missing the opportunity to exploit many of the benefits that composites could provide.

It is becoming increasingly important for novel applications to exploit the capabilities that composite laminates offer by either increasing structural efficiency or by creating novel functionality. For instance, parts made from unsymmetric stacking sequences have been rarely used, because they may introduce several structural couplings and because they may develop internal stresses and warp when cooling down from cure to room temperature. Nonetheless, these or similar phenomena offer great capabilities for novel concepts to be used in emerging research fields such as elastic tailoring and morphing structures [1].

To exploit these capabilities it is crucially important to fully understand the structural behavior of the materials and to examine all sources of anisotropy. The aim of this paper is to gather the understanding necessary to design materials and to obtain tailored structural responses of general shells. Particular attention is given to the relationship between curvatures and stiffness coefficients.

Shell structures have been widely used in engineering applications. The literature offers a variety of theories for both general elasticity problems and particular design purposes. Each theory or analysis has been developed starting from a common point: namely, the differential equations of elastic equilibrium. However, they may differ greatly, depending on the different purpose-driven assumptions and approximations used. Furthermore, despite the availability of a huge variety of papers dedicated to the study of most shell-related structural phenomena, literature almost exclusively applies to the analysis of shells of practical and common use in engineering. Therefore, most published work has been concerned specifically with simple shapes such as cylinders, spheres, cones, or, more generally, shells having small ratios of thickness to radius of

Presented as Paper 2186 at the 49th AIAA/ASME/ASCE/AHS/ASC Structures, Structural Dynamics, and Materials Conference, Schaumburg, IL, 7–10 April 2008; received 10 October 2008; accepted for publication 10 December 2008.

*Ph.D. Student, Department of Aerospace Engineering. Student Member AIAA.

†Reader, Department of Aerospace Engineering. Member AIAA.

curvature. Under this assumption, the effect of the curvature on stiffnesses is often negligible [2].

Comprehensive literature reviews on the mechanics of laminated anisotropic shells can be found in recent papers by Qatu [2] and Toorani and Lakis [3]. Survey articles often emphasize that shear deformations and rotary inertia effects are generally more important for composites than for isotropic materials. Interestingly, Qatu [4,5] showed that neglecting the geometric terms $1 + \zeta/R_i$, in addition to leading to stress resultants that contradict the equations of equilibrium [6], may entail errors of the same order of magnitude as those introduced by Kirchhoff–Love's first approximation. Furthermore, independently and with a different approach, Voyiadjis and Shi [7] and Voyiadjis and Woelke [8] showed, with their work on isotropic shells, that curvature has a significant effect on shell elasticity. They found that the effect of initial curvature on stress resultants and couples is, in general, not negligible. In the present formulation, the term $1 + \zeta/R_i$ is integrated exactly. It will be shown that this procedure provides precise relationships between the stiffness coefficients and shell curvatures and, notably, the influence that these relationships has on both linear and nonlinear structural phenomena.

For all of the aforementioned reasons, the current work attempts to develop a novel model describing shell-like two-dimensional structures. A first-order shear deformation theory (FSDT) for anisotropic, multilayered, deep, and thick shells is presented. It is based on work by Reddy [9,10] for thin, doubly curved, shallow shells. It is the current aim to further develop that work to shells of general shape by following Qatu's [4,5] recommendations and including the effects of geometrically nonlinear deformations, as described by Novozhilov [11,12].

In an attempt to be as general as possible, the model takes into account full anisotropy, general shell geometry, and nonlinear and transverse shear deformations. Inconsistencies that were common in many of the past theories have been considered and overcome [6,9,10,13–15].

The field equations are expressed in curvilinear coordinates lying on the shell's middle surface. For the sake of simplicity, this net is taken to be coincident with the surfaces' principal curves (sometimes called lines of curvature). A novel expression for the stiffness matrix is presented. It is also shown that many of the stiffness coupling terms and the strain components are strongly dependent on the shape of the structure.

Finally, it is noted that there have been a great number of technical papers on the theory of shells in the last century. Those of particular interest, which are in addition to those already mentioned, are detailed in [16–40].

II. Theoretical Development

In the following sections, the theoretical development leading from the governing field equations to the analytical solution (namely, the load-displacement equations for shell structures) are presented.

The usual assumptions are followed:

1) There is linear elastic behavior of the material.

2) The transverse normal fibers are not elongated.

3) The normal stress in the thickness direction is negligible compared with other stresses in the same direction.

4) The Kirchhoff–Love hypothesis is relaxed, and so those elemental fibers that were straight and normal to the middle plane before deformation remain straight but are no longer normal to that plane after deformation.

A. Geometry of Curved Surfaces

The previous assumptions allow the mechanics of the shell to be described as a two-dimensional problem. The structural behavior of the generic shell is then reduced to a function of its middle surface. It is assumed that the middle surface of the shell structure is described by the curvilinear coordinate system (ξ_1, ξ_2, ζ) [10], where ξ_1 and ξ_2 are coordinates describing the position on the middle surface, and ζ is the coordinate in the thickness direction. This being the case, points on the middle surface and in an arbitrary position are described, respectively, by vectors $\mathbf{r} = \mathbf{r}(\xi_1, \xi_2, 0)$ and $\mathbf{R} = \mathbf{R}(\xi_1, \xi_2, \zeta)$.

The metric properties of a surface are completely described by the first fundamental form. It determines the length of an element of middle surface as

$$ds^2 = d\mathbf{r} \cdot d\mathbf{r} = E d\xi_1^2 + 2F d\xi_1 d\xi_2 + G d\xi_2^2 \qquad (1)$$

The coefficients in Eq. (1) represent the elements of the surface metric tensor and are defined as

$$E = \frac{\partial \mathbf{r}}{\partial \xi_1} \cdot \frac{\partial \mathbf{r}}{\partial \xi_1}, \qquad F = \frac{\partial \mathbf{r}}{\partial \xi_1} \cdot \frac{\partial \mathbf{r}}{\partial \xi_2}, \qquad G = \frac{\partial \mathbf{r}}{\partial \xi_2} \cdot \frac{\partial \mathbf{r}}{\partial \xi_2} \qquad (2)$$

In curvilinear coordinate systems, the quantities $a_1 = \sqrt{E}$ and $a_2 = \sqrt{G}$ represent the length of the vectors tangent to curves of constant ξ_1 and ξ_2 and are called scale factors, and F is proportional to the angle χ between the tangent vectors and is equal to $a_1 a_2 \cos \chi$. Similarly, A_1 and A_2, the so-called Lamé coefficients, have analogous meanings for points through the thickness. Provided that R_1 and R_2 denote the normal radii of curvature of the middle surface, then

$$A_1 = a_1\left(1 + \frac{\zeta}{R_1}\right), \qquad A_2 = a_2\left(1 + \frac{\zeta}{R_2}\right) \qquad (3)$$

The first fundamental form defines a family of surfaces with the same metric. The surface itself is fully determined by also considering the coefficients of the second fundamental form. These coefficients are related to the surface curvature and are defined as

$$L = \frac{\partial^2 \mathbf{r}}{\partial \xi_1^2} \cdot \mathbf{n}, \qquad M = \frac{\partial^2 \mathbf{r}}{\partial \xi_1 \partial \xi_2} \cdot \mathbf{n}, \qquad N = \frac{\partial^2 \mathbf{r}}{\partial \xi_2^2} \cdot \mathbf{n} \qquad (4)$$

where $\mathbf{n}$ is the unit vector normal to the middle surface and is defined as

$$\mathbf{n} = \left(\frac{\partial \mathbf{r}}{\partial \xi_1} \times \frac{\partial \mathbf{r}}{\partial \xi_2}\right) \Big/ a_1 a_2 \qquad (5)$$

For the sake of simplicity, in the following formulation, the elasticity equations will be expressed in the curvilinear coordinates system defined by the surface's principal curves (i.e., curves for which the tangent is always coincident with one of the principal directions). It is then assumed that the coordinate lines are both orthogonal ($F = 0$) and conjugate ($M = 0$). This can be done without losing generality. Although the coefficients of the fundamental forms depend on the surface parametric definition that is adopted, finding a coordinate transformation to fulfill the preceding requirements (i.e., $F = M = 0$) is not a trivial matter. However, in the theory of surfaces, it has been proved that every surface can be referred to its principal lines and that they are uniquely determined (see [4,6,16] for further details).

Here, a common analytical method to find principal curves is briefly described. It exploits the concept of the velocity vector of a curve. Let $\mathbf{x}$ be a surface defined in $\mathbb{R}^3$ and let $\boldsymbol{\alpha}(t) = \mathbf{x}(f(t), g(t))$ be a curve lying on it. Then $\boldsymbol{\alpha}$ is a principal curve if and only if the following differential equation [16] holds:

$$(ME - LF)\left(\frac{df}{dt}\right)^2 + (NE - LG)\frac{df}{dt}\frac{dg}{dt} + (NF - MG)\left(\frac{dg}{dt}\right)^2 = 0 \qquad (6)$$

In fact, note that for certain surfaces, there is a more convenient method to find principal curves based on the notion of a triply orthogonal system of surfaces [16].

B. Strain-Displacement Relations

The nonlinear strains, under the hypothesis of small relative deformations, are defined in curvilinear coordinates [11] as

$$
\begin{aligned}
\varepsilon_{11} &= e_{11} + \tfrac{1}{2}[e_{11}^2 + (\tfrac{1}{2}e_{12} + \omega_3)^2 + (\tfrac{1}{2}e_{13} - \omega_2)^2] \\
\varepsilon_{22} &= e_{22} + \tfrac{1}{2}[e_{22}^2 + (\tfrac{1}{2}e_{12} - \omega_3)^2 + (\tfrac{1}{2}e_{23} + \omega_1)^2] \\
\varepsilon_{12} &= e_{12} + e_{11}(\tfrac{1}{2}e_{12} - \omega_3) + e_{22}(\tfrac{1}{2}e_{12} + \omega_3) \\
&\quad + (\tfrac{1}{2}e_{13} - \omega_2)(\tfrac{1}{2}e_{23} + \omega_1) \\
\varepsilon_{13} &= e_{13} + e_{11}(\tfrac{1}{2}e_{13} + \omega_2) + (\tfrac{1}{2}e_{12} + \omega_3)(\tfrac{1}{2}e_{23} - \omega_1) \\
\varepsilon_{23} &= e_{23} + e_{22}(\tfrac{1}{2}e_{23} - \omega_1) + (\tfrac{1}{2}e_{12} - \omega_3)(\tfrac{1}{2}e_{13} + \omega_2)
\end{aligned} \tag{7}
$$

The expressions in Eqs. (7) are a nonlinear combination of those elements that fully describe continuum deformations under the hypothesis of small displacements and rotations: that is, in the classical linear theory of elasticity (in which $\varepsilon_{ij} \approx e_{ij}$). It is shown in several works [2–15] that linear deformations in orthogonal curvilinear coordinates are described using the relationships

$$
\begin{aligned}
e_{11} &= \frac{1}{A_1}\left(\frac{\partial u}{\partial \xi_1} + \frac{1}{A_2}\frac{\partial A_1}{\partial \xi_2}v + \frac{A_1}{R_1}w\right) = \frac{1}{A_1}\left(\frac{\partial u}{\partial \xi_1} + \frac{1}{a_2}\frac{\partial a_1}{\partial \xi_2}v + \frac{a_1}{R_1}w\right) \\
e_{22} &= \frac{1}{A_2}\left(\frac{\partial v}{\partial \xi_2} + \frac{1}{A_1}\frac{\partial A_2}{\partial \xi_1}u + \frac{A_2}{R_2}w\right) = \frac{1}{A_2}\left(\frac{\partial v}{\partial \xi_2} + \frac{1}{a_1}\frac{\partial a_2}{\partial \xi_1}u + \frac{a_2}{R_2}w\right) \\
e_{12} &= \frac{A_2}{A_1}\frac{\partial}{\partial \xi_1}\left(\frac{v}{A_2}\right) + \frac{A_1}{A_2}\frac{\partial}{\partial \xi_2}\left(\frac{u}{A_1}\right) \\
&= \frac{1}{A_1}\left(\frac{\partial v}{\partial \xi_1} - \frac{1}{a_2}\frac{\partial a_1}{\partial \xi_2}u\right) + \frac{1}{A_2}\left(\frac{\partial u}{\partial \xi_2} - \frac{1}{a_1}\frac{\partial a_2}{\partial \xi_1}v\right) \\
e_{13} &= A_1\frac{\partial}{\partial \zeta}\left(\frac{u}{A_1}\right) + \frac{1}{A_1}\frac{\partial w}{\partial \xi_1} = \frac{\partial u}{\partial \zeta} + \frac{1}{1+\frac{\zeta}{R_1}}\left(\frac{1}{a_1}\frac{\partial w}{\partial \xi_1} - \frac{u}{R_1}\right) \\
e_{23} &= \frac{1}{A_2}\frac{\partial w}{\partial \xi_2} + A_2\frac{\partial}{\partial \zeta}\left(\frac{v}{A_2}\right) = \frac{\partial v}{\partial \zeta} + \frac{1}{1+\frac{\zeta}{R_2}}\left(\frac{1}{a_2}\frac{\partial w}{\partial \xi_2} - \frac{v}{R_2}\right) \\
2\omega_1 &= \frac{1}{A_2}\left[\frac{\partial w}{\partial \xi_2} - \frac{\partial}{\partial \zeta}(A_2 v)\right] = -\frac{\partial v}{\partial \zeta} + \frac{1}{1+\frac{\zeta}{R_2}}\left(\frac{1}{a_2}\frac{\partial w}{\partial \xi_2} - \frac{v}{R_2}\right) \\
2\omega_2 &= \frac{1}{A_1}\left[\frac{\partial}{\partial \zeta}(A_1 u) - \frac{\partial w}{\partial \xi_1}\right] = \frac{\partial u}{\partial \zeta} - \frac{1}{1+\frac{\zeta}{R_1}}\left(\frac{1}{a_1}\frac{\partial w}{\partial \xi_1} - \frac{u}{R_1}\right) \\
2\omega_3 &= \frac{1}{A_1 A_2}\left[\frac{\partial}{\partial \xi_1}(A_2 v) - \frac{\partial}{\partial \xi_2}(A_1 u)\right] \\
&= \frac{1}{A_1}\left(\frac{\partial v}{\partial \xi_1} - \frac{1}{a_2}\frac{\partial a_1}{\partial \xi_2}u\right) - \frac{1}{A_2}\left(\frac{\partial u}{\partial \xi_2} - \frac{1}{a_1}\frac{\partial a_2}{\partial \xi_1}v\right)
\end{aligned} \tag{8}
$$

According to the hypothesis described at the beginning of Sec. II, the surface displacements u, v and w are assumed to be

$$
\begin{aligned}
u(\xi_1, \xi_2, \zeta, t) &= u_0(\xi_1, \xi_2, t) + \zeta\phi_1(\xi_1, \xi_2, t) \\
v(\xi_1, \xi_2, \zeta, t) &= v_0(\xi_1, \xi_2, t) + \zeta\phi_2(\xi_1, \xi_2, t) \\
w(\xi_1, \xi_2, \zeta, t) &= w_0(\xi_1, \xi_2, t)
\end{aligned} \tag{9}
$$

Substituting Eqs. (9) into Eqs. (8) enables the linear strains to be separated into terms (or components) depending on displacements and rotations of the middle surface:

$$e_1^0 = \frac{1}{a_1}\left(\frac{\partial u_0}{\partial \xi_1} + \frac{v_0}{a_2}\frac{\partial a_1}{\partial \xi_2} + \frac{a_1}{R_1}w_0\right)$$

$$e_2^0 = \frac{1}{a_2}\left(\frac{\partial v_0}{\partial \xi_2} + \frac{u_0}{a_1}\frac{\partial a_2}{\partial \xi_1} + \frac{a_2}{R_2}w_0\right)$$

$$\omega_1^0 = \frac{1}{a_1}\left(\frac{\partial v_0}{\partial \xi_1} - \frac{u_0}{a_2}\frac{\partial a_1}{\partial \xi_2}\right), \qquad \omega_2^0 = \frac{1}{a_2}\left(\frac{\partial u_0}{\partial \xi_2} - \frac{v_0}{a_1}\frac{\partial a_2}{\partial \xi_1}\right)$$

$$e_4^0 = \frac{1}{a_2}\left(\frac{\partial w_0}{\partial \xi_2} + a_2\phi_2 - \frac{a_2}{R_2}v_0\right)$$

$$e_5^0 = \frac{1}{a_1}\left(\frac{\partial w_0}{\partial \xi_1} + a_1\phi_1 - \frac{a_1}{R_1}u_0\right)$$

$$\kappa_1^0 = \frac{1}{a_2}\left(\frac{\partial w_0}{\partial \xi_2} - \frac{a_2}{R_2}v_0 - a_2\phi_2\right)$$

$$\kappa_2^0 = \frac{1}{a_1}\left(-\frac{\partial w_0}{\partial \xi_1} + \frac{a_1}{R_1}u_0 + a_1\phi_1\right)$$

$$e_1^1 = \frac{1}{a_1}\left(\frac{\partial \phi_1}{\partial \xi_1} + \frac{\phi_2}{a_2}\frac{\partial a_1}{\partial \xi_2}\right), \qquad e_2^1 = \frac{1}{a_2}\left(\frac{\partial \phi_2}{\partial \xi_2} + \frac{\phi_1}{a_1}\frac{\partial a_2}{\partial \xi_1}\right)$$

$$\omega_1^1 = \frac{1}{a_1}\left(\frac{\partial \phi_2}{\partial \xi_1} - \frac{\phi_1}{a_2}\frac{\partial a_1}{\partial \xi_2}\right), \qquad \omega_2^1 = \frac{1}{a_2}\left(\frac{\partial \phi_1}{\partial \xi_2} - \frac{\phi_2}{a_1}\frac{\partial a_2}{\partial \xi_1}\right)$$

$$\kappa_1^1 = -2\frac{\phi_2}{R_2}, \qquad \kappa_2^1 = +2\frac{\phi_1}{R_1} \tag{10}$$

where superscripts 0 and 1 refer to in-surface and out-of-surface components of linear deformations, respectively. Substituting Eqs. (10) into Eqs. (7), the following expressions for nonlinear strains are obtained:

$$
\begin{aligned}
\varepsilon_{11} &= \frac{e_1^0 + \zeta e_1^1}{1 + \zeta/R_1} + \frac{1}{2(1 + \zeta/R_1)^2} \\
&\quad \times \left[(e_1^0 + \zeta e_1^1)^2 + (\omega_1^0 + \zeta\omega_1^1)^2 + \frac{1}{4}(e_5^0 - \kappa_2^0 - \zeta\kappa_2^1)^2\right] \\
\varepsilon_{22} &= \frac{e_2^0 + \zeta e_2^1}{1 + \zeta/R_2} + \frac{1}{2(1 + \zeta/R_2)^2} \\
&\quad \times \left[(e_2^0 + \zeta e_2^1)^2 + (\omega_2^0 + \zeta\omega_2^1)^2 + \frac{1}{4}(e_4^0 + \kappa_1^0 + \zeta\kappa_1^1)^2\right] \\
\varepsilon_{12} &= \frac{\omega_1^0 + \zeta\omega_1^1}{1 + \zeta/R_1} + \frac{\omega_2^0 + \zeta\omega_2^1}{1 + \zeta/R_2} + \frac{1}{(1 + \zeta/R_1)(1 + \zeta/R_2)} \\
&\quad \times \left[(e_1^0 + \zeta e_1^1)(\omega_2^0 + \zeta\omega_2^1) + (e_2^0 + \zeta e_2^1)(\omega_1^0 + \zeta\omega_1^1)\right. \\
&\quad \left. + \frac{1}{4}(e_5^0 - \kappa_2^0 - \zeta\kappa_2^1)(e_4^0 + \kappa_1^0 + \zeta\kappa_1^1)\right] \\
\varepsilon_{13} &= \frac{e_5^0}{1 + \zeta/R_1} + \frac{1}{2}\left[\frac{(e_1^0 + \zeta e_1^1)(e_5^0 + \kappa_2^0 + \zeta\kappa_2^1)}{(1 + \zeta/R_1)^2}\right. \\
&\quad \left. + \frac{(\omega_1^0 + \zeta\omega_1^1)(e_4^0 - \kappa_1^0 - \zeta\kappa_1^1)}{(1 + \zeta/R_1)(1 + \zeta/R_2)}\right] \\
\varepsilon_{23} &= \frac{e_4^0}{1 + \zeta/R_2} + \frac{1}{2}\left[\frac{(e_2^0 + \zeta e_2^1)(e_4^0 - \kappa_1^0 - \zeta\kappa_1^1)}{(1 + \zeta/R_2)^2}\right. \\
&\quad \left. + \frac{(\omega_2^0 + \zeta\omega_2^1)(e_5^0 + \kappa_2^0 + \zeta\kappa_2^1)}{(1 + \zeta/R_1)(1 + \zeta/R_2)}\right]
\end{aligned} \tag{11}
$$

Equation (7) or Eq. (11) are generally valid for small relative deformations, but in some practical problems, this level of accuracy might be not necessary. Simplified expressions (even though less general) can be found in [11] under the hypothesis of small rotations or in [10] with von Kármán nonlinearities. The proposed model can be simplified accordingly.

C. Stress Resultants

The stress resultants acting on the shell element are obtained by integrating each stress over the thickness [10] as

$$\begin{Bmatrix} N_{11} \\ N_{12} \\ Q_{11} \\ M_{11} \\ M_{12} \end{Bmatrix} = \int_{-h/2}^{h/2} \left(1 + \frac{\zeta}{R_2}\right) \begin{Bmatrix} \sigma_1 \\ \sigma_6 \\ \sigma_5 K_s \\ \zeta\sigma_1 \\ \zeta\sigma_6 \end{Bmatrix} \mathrm{d}\zeta$$

$$\begin{Bmatrix} N_{22} \\ N_{21} \\ Q_{22} \\ M_{22} \\ M_{21} \end{Bmatrix} = \int_{-h/2}^{h/2} \left(1 + \frac{\zeta}{R_1}\right) \begin{Bmatrix} \sigma_2 \\ \sigma_6 \\ \sigma_4 K_s \\ \zeta\sigma_2 \\ \zeta\sigma_6 \end{Bmatrix} \mathrm{d}\zeta \tag{12}$$

where K_s is the shear correction factor used to adjust the discrepancy between the true variation of the transverse shear and that which has been imposed.

The definition of the stress resultants is a key feature of the present formulation and merits further discussion. In many shallow thin shell theories, the term $1 + \zeta/R_i$, which is due to the integration over the thickness of a curved section, has been ignored and the stiffness coefficients have been calculated as for flat plates {henceforth, we will refer to this as plate approximation (P.A.) [4]}. This led to fairly good results, even though it was clear that the artificially achieved symmetry of the resultants $M_{ij} = M_{ji}$ and $N_{ij} = N_{ji}$ contradicts drilling equilibrium [6]. This inconsistency was often overcome by expanding the term in a geometric series, thus restoring the relationship

$$\frac{M_{21}}{R_2} - \frac{M_{12}}{R_1} + N_{21} - N_{12} = 0 \tag{13}$$

which derives from the exact definition of resultants and identically satisfies one of the equilibrium equations. Alternatively, some researchers including the effects of $1 + \zeta/R_i$ suggested the use of modified stress resultants to ensure symmetry [13–15,17].

As already established, transverse shear deformations may have a significant role in the mechanics of thick laminated composite structures, and their effects may need to be included in the analysis of shells. According to [4], the error introduced by neglecting them is of the same order of magnitude as that created by approximating $1 + \zeta/R_i$ to unity.

For consistency purposes, the integration of Eqs. (12) has to then be carried out exactly. By so doing, we will find that curvatures are a source of anisotropy (coupling between membrane and flexural effects), even for isotropic materials, and that the stiffness coefficients are not constants, as when calculated with the flat-plate approximation, but functions of the curvatures. Reference [4] also shows that the results of the study of linear phenomena using exact stiffness coefficients are generally more accurate when compared with those of FSDT or even higher-order shear deformation theory. This degree of accuracy is due to the different way in which the stiffness matrix is calculated. It will be shown here that this difference will lead to appreciably different values of strain components. It is thus argued that maintaining the accurate expression of the stresses resultant will affect nonlinear effects such as buckling or postbuckling phenomena.

D. Constitutive Relations

Suppose that the shell structure is composed of N layers. For each layer, the constitutive law is

$$\begin{Bmatrix} \sigma_1 \\ \sigma_2 \\ \sigma_4 \\ \sigma_5 \\ \sigma_6 \end{Bmatrix} = \begin{bmatrix} \bar{Q}_{11} & \bar{Q}_{12} & 0 & 0 & \bar{Q}_{16} \\ \bar{Q}_{12} & \bar{Q}_{22} & 0 & 0 & \bar{Q}_{26} \\ 0 & 0 & \bar{Q}_{44} & \bar{Q}_{45} & 0 \\ 0 & 0 & \bar{Q}_{45} & \bar{Q}_{55} & 0 \\ \bar{Q}_{16} & \bar{Q}_{26} & 0 & 0 & \bar{Q}_{66} \end{bmatrix} \left(\begin{Bmatrix} \varepsilon_1 \\ \varepsilon_2 \\ \varepsilon_4 \\ \varepsilon_5 \\ \varepsilon_6 \end{Bmatrix}^L + \begin{Bmatrix} \varepsilon_1 \\ \varepsilon_2 \\ \varepsilon_4 \\ \varepsilon_5 \\ \varepsilon_6 \end{Bmatrix}^{\mathrm{NL}} \right) \tag{14}$$

For convenience, in Eq. (14), the strain vector is split in two parts in which the superscripts L and NL mean linear and nonlinear, respectively. Similarly, the stress resultants are presented as a sum of two vectors corresponding to distributed forces and moments resulting from linear and nonlinear strains so that, for example, N_{11} will be the sum of N_{11}^L and N_{11}^{NL}.

By means of Eqs. (7), one can write

$$\begin{Bmatrix} \varepsilon_1 \\ \varepsilon_2 \\ \varepsilon_4 \\ \varepsilon_5 \\ \varepsilon_6 \end{Bmatrix}^L = \begin{Bmatrix} e_{11} \\ e_{22} \\ e_{23} \\ e_{13} \\ e_{12} \end{Bmatrix} \tag{15}$$

$$\begin{Bmatrix} \varepsilon_1 \\ \varepsilon_2 \\ \varepsilon_4 \\ \varepsilon_5 \\ \varepsilon_6 \end{Bmatrix}^{\mathrm{NL}} = \begin{Bmatrix} \frac{1}{2}[e_{11}^2 + (\frac{1}{2}e_{12} + \omega_3)^2 + (\frac{1}{2}e_{13} - \omega_2)^2] \\ \frac{1}{2}[e_{22}^2 + (\frac{1}{2}e_{12} - \omega_3)^2 + (\frac{1}{2}e_{23} + \omega_1)^2] \\ e_{22}(\frac{1}{2}e_{23} - \omega_1) + (\frac{1}{2}e_{12} - \omega_3)(\frac{1}{2}e_{13} + \omega_2) \\ e_{11}(\frac{1}{2}e_{13} + \omega_2) + (\frac{1}{2}e_{12} + \omega_3)(\frac{1}{2}e_{23} - \omega_1) \\ e_{11}(\frac{1}{2}e_{12} - \omega_3) + e_{22}(\frac{1}{2}e_{12} + \omega_3) + (\frac{1}{2}e_{13} - \omega_2)(\frac{1}{2}e_{23} + \omega_1) \end{Bmatrix} \tag{16}$$

Substituting Eq. (14) back into Eqs. (12) and integrating the resulting expressions, it is then possible to obtain the laminate constitutive relations reported in Eqs. (17–19) and (26–28).

E. Laminate Stiffness Matrix Corresponding to Linear Strains

The constitutive equations are

$$\begin{Bmatrix} N_{11} \\ N_{12} \\ N_{22} \\ N_{21} \end{Bmatrix}^L = \begin{bmatrix} A_{11} & A'_{16} & A_{12} & A_{16} \\ A'_{16} & A'_{66} & A_{26} & A_{66} \\ A_{12} & A_{26} & A_{22} & A''_{26} \\ A_{16} & A_{66} & A''_{26} & A''_{66} \end{bmatrix} \begin{Bmatrix} e_1^0 \\ \omega_1^0 \\ e_2^0 \\ \omega_2^0 \end{Bmatrix} + \begin{bmatrix} B_{11} & B'_{16} & B_{12} & B_{16} \\ B'_{16} & B'_{66} & B_{26} & B_{66} \\ B_{12} & B_{26} & B_{22} & B''_{26} \\ B_{16} & B_{66} & B''_{26} & B''_{66} \end{bmatrix} \begin{Bmatrix} e_1^1 \\ \omega_1^1 \\ e_2^1 \\ \omega_2^1 \end{Bmatrix} \tag{17}$$

$$\begin{Bmatrix} M_{11} \\ M_{12} \\ M_{22} \\ M_{21} \end{Bmatrix}^L = \begin{bmatrix} B_{11} & B'_{16} & B_{12} & B_{16} \\ B'_{16} & B'_{66} & B_{26} & B_{66} \\ B_{12} & B_{26} & B_{22} & B''_{26} \\ B_{16} & B_{66} & B''_{26} & B''_{66} \end{bmatrix} \begin{Bmatrix} e_1^0 \\ \omega_1^0 \\ e_2^0 \\ \omega_2^0 \end{Bmatrix} + \begin{bmatrix} D_{11} & D'_{16} & D_{12} & D_{16} \\ D'_{16} & D'_{66} & D_{26} & D_{66} \\ D_{12} & D_{26} & D_{22} & D''_{26} \\ D_{16} & D_{66} & D''_{26} & D''_{66} \end{bmatrix} \begin{Bmatrix} e_1^1 \\ \omega_1^1 \\ e_2^1 \\ \omega_2^1 \end{Bmatrix} \tag{18}$$

$$\begin{Bmatrix} Q_{22} \\ Q_{11} \end{Bmatrix}^L = K_s \begin{bmatrix} A_{44} & A_{45} \\ A_{45} & A_{55} \end{bmatrix} \begin{Bmatrix} e_4^0 \\ e_5^0 \end{Bmatrix} \tag{19}$$

or, in a more compact form,

$$\begin{Bmatrix} N_{11} \\ N_{12} \\ Q_{22} \\ N_{22} \\ N_{21} \\ Q_{11} \\ M_{11} \\ M_{12} \\ M_{22} \\ M_{21} \end{Bmatrix}^{L} = \begin{bmatrix} A_{11} & A'_{16} & 0 & A_{12} & A_{16} & 0 & B_{11} & B'_{16} & B_{12} & B_{16} \\ A'_{16} & A'_{66} & 0 & A_{26} & A_{66} & 0 & B'_{16} & B'_{66} & B_{26} & B_{66} \\ 0 & 0 & K_s A_{44} & 0 & 0 & K_s A_{45} & 0 & 0 & 0 & 0 \\ A_{12} & A_{26} & 0 & A_{22} & A''_{26} & 0 & B_{12} & B_{26} & B_{22} & B''_{26} \\ A_{16} & A_{66} & 0 & A''_{26} & A''_{66} & 0 & B_{16} & B_{66} & B''_{26} & B''_{66} \\ 0 & 0 & K_s A_{45} & 0 & 0 & K_s A_{55} & 0 & 0 & 0 & 0 \\ B_{11} & B'_{16} & 0 & B_{12} & B_{16} & 0 & D_{11} & D'_{16} & D_{12} & D_{16} \\ B'_{16} & B'_{66} & 0 & B_{26} & B_{66} & 0 & D'_{16} & D'_{66} & D_{26} & D_{66} \\ B_{12} & B_{26} & 0 & B_{22} & B''_{26} & 0 & D_{12} & D_{26} & D_{22} & D''_{26} \\ B_{16} & B_{66} & 0 & B''_{26} & B''_{66} & 0 & D_{16} & D_{66} & D''_{26} & D''_{66} \end{bmatrix} \times \begin{Bmatrix} e_1^0 \\ \omega_1^0 \\ e_4^0 \\ e_2^0 \\ \omega_2^0 \\ e_5^0 \\ e_1^1 \\ \omega_1^1 \\ e_2^1 \\ \omega_2^1 \end{Bmatrix} \tag{20}$$

The elements of Eqs. (17–20), which are due to the linear part of the strain components, are calculated using

$$\underline{A} = \begin{bmatrix} A_{11} & A'_{16} & A_{12} & A_{16} \\ A'_{16} & A'_{66} & A_{26} & A_{66} \\ A_{12} & A_{26} & A_{22} & A''_{26} \\ A_{16} & A_{66} & A''_{26} & A''_{66} \end{bmatrix} = \sum_{k=1}^{N} \begin{bmatrix} a^L_{R_1}\bar{Q}_{11} & a^L_{R_1}\bar{Q}_{16} & c^L\bar{Q}_{12} & c^L\bar{Q}_{16} \\ a^L_{R_1}\bar{Q}_{16} & a^L_{R_1}\bar{Q}_{66} & c^L\bar{Q}_{26} & c^L\bar{Q}_{66} \\ c^L\bar{Q}_{12} & c^L\bar{Q}_{16} & a^L_{R_2}\bar{Q}_{22} & a^L_{R_2}\bar{Q}_{26} \\ c^L\bar{Q}_{26} & c^L\bar{Q}_{66} & a^L_{R_2}\bar{Q}_{26} & a^L_{R_2}\bar{Q}_{66} \end{bmatrix}^{(k)} \tag{21}$$

$$\underline{B} = \begin{bmatrix} B_{11} & B'_{16} & B_{12} & B_{16} \\ B'_{16} & B'_{66} & B_{26} & B_{66} \\ B_{12} & B_{26} & B_{22} & B''_{26} \\ B_{16} & B_{66} & B''_{26} & B''_{66} \end{bmatrix} = \sum_{k=1}^{N} \begin{bmatrix} b^L_{R_1}\bar{Q}_{11} & b^L_{R_1}\bar{Q}_{16} & d^L\bar{Q}_{12} & d^L\bar{Q}_{16} \\ b^L_{R_1}\bar{Q}_{16} & b^L_{R_1}\bar{Q}_{66} & d^L\bar{Q}_{26} & d^L\bar{Q}_{66} \\ d^L\bar{Q}_{12} & d^L\bar{Q}_{16} & b^L_{R_2}\bar{Q}_{22} & b^L_{R_2}\bar{Q}_{26} \\ d^L\bar{Q}_{26} & d^L\bar{Q}_{66} & b^L_{R_2}\bar{Q}_{26} & b^L_{R_2}\bar{Q}_{66} \end{bmatrix}^{(k)} \tag{22}$$

$$\underline{D} = \begin{bmatrix} D_{11} & D'_{16} & D_{12} & D_{16} \\ D'_{16} & D'_{66} & D_{26} & D_{66} \\ D_{12} & D_{26} & D_{22} & D''_{26} \\ D_{16} & D_{66} & D''_{26} & D''_{66} \end{bmatrix} = \sum_{k=1}^{N} \begin{bmatrix} e^L_{R_1}\bar{Q}_{11} & e^L_{R_1}\bar{Q}_{16} & f^L\bar{Q}_{12} & f^L\bar{Q}_{16} \\ e^L_{R_1}\bar{Q}_{16} & e^L_{R_1}\bar{Q}_{66} & f^L\bar{Q}_{26} & f^L\bar{Q}_{66} \\ f^L\bar{Q}_{12} & f^L\bar{Q}_{16} & e^L_{R_2}\bar{Q}_{22} & e^L_{R_2}\bar{Q}_{26} \\ f^L\bar{Q}_{26} & f^L\bar{Q}_{66} & e^L_{R_2}\bar{Q}_{26} & e^L_{R_2}\bar{Q}_{66} \end{bmatrix}^{(k)} \tag{23}$$

$$\begin{bmatrix} A_{44} & A_{45} \\ A_{45} & A_{55} \end{bmatrix} = \sum_{k=1}^{N} \begin{bmatrix} a^L_{R_2}\bar{Q}_{44} & c^L\bar{Q}_{45} \\ c^L\bar{Q}_{45} & a^L_{R_1}\bar{Q}_{55} \end{bmatrix}^{(k)} \tag{24}$$

and

$$\begin{aligned} a^L_{R_1} &= \frac{R_1}{R_2}\left[(\zeta_{k+1}-\zeta_k) + (R_2 - R_1)\,\ell n\left(\frac{R_1+\zeta_{k+1}}{R_1+\zeta_k}\right)\right] \\ b^L_{R_1} &= \frac{R_1}{R_2}\left[\frac{1}{2}(\zeta^2_{k+1}-\zeta^2_k) + (R_2-R_1)(\zeta_{k+1}-\zeta_k) \right. \\ &\quad \left. - R_1(R_2-R_1)\,\ell n\left(\frac{R_1+\zeta_{k+1}}{R_1+\zeta_k}\right)\right] \\ c^L &= (\zeta_{k+1}-\zeta_k) \qquad d^L = \frac{1}{2}(\zeta^2_{k+1}-\zeta^2_k) \\ e^L_{R_1} &= \frac{R_1}{R_2}\left[\frac{1}{3}(\zeta^3_{k+1}-\zeta^3_k) + \frac{1}{2}(R_2-R_1)(\zeta^2_{k+1}-\zeta^2_k) \right. \\ &\quad \left. - R_1(R_2-R_1)(\zeta_{k+1}-\zeta_k) + R_1^2(R_2-R_1)\,\ell n\left(\frac{R_1+\zeta_{k+1}}{R_1+\zeta_k}\right)\right] \\ f^L &= \frac{1}{3}(\zeta^3_{k+1}-\zeta^3_k) \end{aligned} \tag{25}$$

Similar coefficients with R_2 as subscript can be obtained by simply interchanging subscripts 1 and 2. Note that symmetry has been achieved by decomposing shear strains into two separate components. Splitting shear strain into two constituent parts allows distinct components for N_{12}, N_{21}, M_{12}, and M_{21} to be retained while allowing both physically meaningful stress components and symmetry for our problem, noting that symmetry is retained via two 4×4 stiffness matrices rather than the conventional 3×3. As such, our formulation is an alternative to that shown in [13–15,17].

F. Laminate Stiffness Matrix Corresponding to Nonlinear Strains

Similarly, it is possible to obtain the part of the constitutive equations due to the nonlinear strains:

$$
\begin{Bmatrix} N_{11} \\ N_{12} \\ N_{22} \\ N_{21} \end{Bmatrix}^{\mathrm{NL}} = \frac{1}{4} \begin{bmatrix} \mathrm{A}_{11} & \mathrm{A}_{12} & \mathrm{A}_{13} \\ \mathrm{A}_{21} & \mathrm{A}_{22} & \mathrm{A}_{23} \\ \mathrm{A}_{31} & \mathrm{A}_{32} & \mathrm{A}_{33} \\ \mathrm{A}_{41} & \mathrm{A}_{42} & \mathrm{A}_{43} \end{bmatrix}
\times \begin{Bmatrix} \frac{1}{2}(4e_1^{02} + 4\omega_1^{02} + e_5^{02} + \kappa_2^{02} - 2e_5^0\kappa_2^0) \\ \frac{1}{2}(4e_2^{02} + 4\omega_2^{02} + e_4^{02} + \kappa_1^{02} + 2e_4^0\kappa_1^0) \\ 4\omega_2^0 e_1^0 + 4\omega_1^0 e_2^0 + e_5^0 e_4^0 + e_5^0\kappa_1^0 - e_4^0\kappa_2^0 - \kappa_1^0\kappa_2^0 \end{Bmatrix}
+ \frac{1}{4} \begin{bmatrix} \Gamma_{11} & \Gamma_{12} & \Gamma_{13} \\ \Gamma_{21} & \Gamma_{22} & \Gamma_{23} \\ \Gamma_{31} & \Gamma_{32} & \Gamma_{33} \\ \Gamma_{41} & \Gamma_{42} & \Gamma_{43} \end{bmatrix}
\times \begin{Bmatrix} 4e_1^0 e_1^1 + 4\omega_1^0\omega_1^1 - e_5^0\kappa_2^1 + \kappa_2^0\kappa_2^1 \\ 4e_2^0 e_2^1 + 4\omega_2^0\omega_2^1 + e_4^0\kappa_1^1 + \kappa_1^0\kappa_1^1 \\ 4(\omega_2^1 e_1^0 + \omega_2^0 e_1^1 + \omega_1^1 e_2^0 + \omega_1^0 e_2^1) + \kappa_1^1(e_5^0 - \kappa_2^0) - \kappa_2^1(e_4^0 + \kappa_1^0) \end{Bmatrix}
+ \frac{1}{4} \begin{bmatrix} \mathrm{B}_{11} & \mathrm{B}_{12} & \mathrm{B}_{13} \\ \mathrm{B}_{21} & \mathrm{B}_{22} & \mathrm{B}_{23} \\ \mathrm{B}_{31} & \mathrm{B}_{32} & \mathrm{B}_{33} \\ \mathrm{B}_{41} & \mathrm{B}_{42} & \mathrm{B}_{43} \end{bmatrix} \begin{Bmatrix} \frac{1}{2}(4e_1^{12} + 4\omega_1^{12} + \kappa_2^{12}) \\ \frac{1}{2}(4e_2^{12} + 4\omega_2^{12} + \kappa_1^{12}) \\ 4\omega_2^1 e_1^1 + 4\omega_1^1 e_2^1 - \kappa_1^1\kappa_2^1 \end{Bmatrix} \tag{26}
$$

$$
\begin{Bmatrix} M_{11} \\ M_{12} \\ M_{22} \\ M_{21} \end{Bmatrix}^{\mathrm{NL}} = \frac{1}{4} \begin{bmatrix} \Gamma_{11} & \Gamma_{12} & \Gamma_{13} \\ \Gamma_{21} & \Gamma_{22} & \Gamma_{23} \\ \Gamma_{31} & \Gamma_{32} & \Gamma_{33} \\ \Gamma_{41} & \Gamma_{42} & \Gamma_{43} \end{bmatrix}
\times \begin{Bmatrix} \frac{1}{2}(4e_1^{02} + 4\omega_1^{02} + e_5^{02} + \kappa_2^{02} - 2e_5^0\kappa_2^0) \\ \frac{1}{2}(4e_2^{02} + 4\omega_2^{02} + e_4^{02} + \kappa_1^{02} + 2e_4^0\kappa_1^0) \\ 4\omega_2^0 e_1^0 + 4\omega_1^0 e_2^0 + e_5^0 e_4^0 + e_5^0\kappa_1^0 - e_4^0\kappa_2^0 - \kappa_1^0\kappa_2^0 \end{Bmatrix}
+ \frac{1}{4} \begin{bmatrix} \mathrm{B}_{11} & \mathrm{B}_{12} & \mathrm{B}_{13} \\ \mathrm{B}_{21} & \mathrm{B}_{22} & \mathrm{B}_{23} \\ \mathrm{B}_{31} & \mathrm{B}_{32} & \mathrm{B}_{33} \\ \mathrm{B}_{41} & \mathrm{B}_{42} & \mathrm{B}_{43} \end{bmatrix}
\times \begin{Bmatrix} 4e_1^0 e_1^1 + 4\omega_1^0\omega_1^1 - e_5^0\kappa_2^1 + \kappa_2^0\kappa_2^1 \\ 4e_2^0 e_2^1 + 4\omega_2^0\omega_2^1 + e_4^0\kappa_1^1 + \kappa_1^0\kappa_1^1 \\ 4(\omega_2^1 e_1^0 + \omega_2^0 e_1^1 + \omega_1^1 e_2^0 + \omega_1^0 e_2^1) + \kappa_1^1(e_5^0 - \kappa_2^0) - \kappa_2^1(e_4^0 + \kappa_1^0) \end{Bmatrix}
+ \frac{1}{4} \begin{bmatrix} \Delta_{11} & \Delta_{12} & \Delta_{13} \\ \Delta_{21} & \Delta_{22} & \Delta_{23} \\ \Delta_{31} & \Delta_{32} & \Delta_{33} \\ \Delta_{41} & \Delta_{42} & \Delta_{43} \end{bmatrix} \begin{Bmatrix} \frac{1}{2}(4e_1^{12} + 4\omega_1^{12} + \kappa_2^{12}) \\ \frac{1}{2}(4e_2^{12} + 4\omega_2^{12} + \kappa_1^{12}) \\ 4\omega_2^1 e_1^1 + 4\omega_1^1 e_2^1 - \kappa_1^1\kappa_2^1 \end{Bmatrix} \tag{27}
$$

and

$$
\begin{Bmatrix} Q_{22} \\ Q_{11} \end{Bmatrix}^{\mathrm{NL}} = \frac{K_s}{2} \begin{bmatrix} \mathrm{E}_{11} & \mathrm{E}_{12} & \mathrm{E}_{13} & \mathrm{E}_{14} \\ \mathrm{E}_{21} & \mathrm{E}_{22} & \mathrm{E}_{23} & \mathrm{E}_{24} \end{bmatrix} \begin{Bmatrix} e_2^0 e_4^0 - e_2^0\kappa_1^0 \\ \omega_2^0 e_5^0 + \omega_2^0\kappa_2^0 \\ e_1^0 e_5^0 + e_1^0\kappa_2^0 \\ \omega_1^0 e_4^0 - \omega_1^0\kappa_1^0 \end{Bmatrix}
+ \frac{K_s}{2} \begin{bmatrix} \mathrm{Z}_{11} & \mathrm{Z}_{12} & \mathrm{Z}_{13} & \mathrm{Z}_{14} \\ \mathrm{Z}_{21} & \mathrm{Z}_{22} & \mathrm{Z}_{23} & \mathrm{Z}_{24} \end{bmatrix} \begin{Bmatrix} e_2^1 e_4^0 - e_2^0\kappa_1^1 - e_2^1\kappa_1^0 \\ \omega_2^0\kappa_2^1 + \omega_2^1 e_5^0 + \omega_2^1\kappa_2^0 \\ e_1^1 e_5^0 + e_1^0\kappa_2^1 + e_1^1\kappa_2^0 \\ \omega_1^1 e_4^0 - \omega_1^0\kappa_1^1 - \omega_1^1\kappa_1^0 \end{Bmatrix}
+ \frac{K_s}{2} \begin{bmatrix} \mathrm{H}_{11} & \mathrm{H}_{12} & \mathrm{H}_{13} & \mathrm{H}_{14} \\ \mathrm{H}_{21} & \mathrm{H}_{22} & \mathrm{H}_{23} & \mathrm{H}_{24} \end{bmatrix} \begin{Bmatrix} -e_2^1\kappa_1^1 \\ \omega_2^1\kappa_2^1 \\ e_1^1\kappa_2^1 \\ -\omega_1^1\kappa_1^1 \end{Bmatrix} \tag{28}
$$

The coefficients of Eqs. (26–28), which are due to the nonlinear part of the strains, are calculated using

$$
\underline{\mathrm{A}} = \begin{bmatrix} \mathrm{A}_{11} & \mathrm{A}_{12} & \mathrm{A}_{13} \\ \mathrm{A}_{21} & \mathrm{A}_{22} & \mathrm{A}_{23} \\ \mathrm{A}_{31} & \mathrm{A}_{32} & \mathrm{A}_{33} \\ \mathrm{A}_{41} & \mathrm{A}_{42} & \mathrm{A}_{43} \end{bmatrix}
= \sum_{k=1}^{N} \begin{bmatrix} \bar{Q}_{11} a_{R_1}^{\mathrm{NL}} & \bar{Q}_{12} d_{R_2}^{\mathrm{NL}} & \bar{Q}_{16} d_{R_1}^{\mathrm{NL}} \\ \bar{Q}_{16} a_{R_1}^{\mathrm{NL}} & \bar{Q}_{26} d_{R_2}^{\mathrm{NL}} & \bar{Q}_{66} d_{R_1}^{\mathrm{NL}} \\ \bar{Q}_{12} d_{R_1}^{\mathrm{NL}} & \bar{Q}_{22} a_{R_2}^{\mathrm{NL}} & \bar{Q}_{26} d_{R_2}^{\mathrm{NL}} \\ \bar{Q}_{16} d_{R_1}^{\mathrm{NL}} & \bar{Q}_{26} a_{R_2}^{\mathrm{NL}} & \bar{Q}_{66} d_{R_2}^{\mathrm{NL}} \end{bmatrix}^{(k)} \tag{29}
$$

$$
\underline{\mathrm{B}} = \begin{bmatrix} \mathrm{B}_{11} & \mathrm{B}_{12} & \mathrm{B}_{13} \\ \mathrm{B}_{21} & \mathrm{B}_{22} & \mathrm{B}_{23} \\ \mathrm{B}_{31} & \mathrm{B}_{32} & \mathrm{B}_{33} \\ \mathrm{B}_{41} & \mathrm{B}_{42} & \mathrm{B}_{43} \end{bmatrix}
= \sum_{k=1}^{N} \begin{bmatrix} \bar{Q}_{11} c_{R_1}^{\mathrm{NL}} & \bar{Q}_{12} f_{R_2}^{\mathrm{NL}} & \bar{Q}_{16} f_{R_1}^{\mathrm{NL}} \\ \bar{Q}_{16} c_{R_1}^{\mathrm{NL}} & \bar{Q}_{26} f_{R_2}^{\mathrm{NL}} & \bar{Q}_{66} f_{R_1}^{\mathrm{NL}} \\ \bar{Q}_{12} f_{R_1}^{\mathrm{NL}} & \bar{Q}_{22} c_{R_2}^{\mathrm{NL}} & \bar{Q}_{26} f_{R_2}^{\mathrm{NL}} \\ \bar{Q}_{16} f_{R_1}^{\mathrm{NL}} & \bar{Q}_{26} c_{R_2}^{\mathrm{NL}} & \bar{Q}_{66} f_{R_2}^{\mathrm{NL}} \end{bmatrix}^{(k)} \tag{30}
$$

$$
\underline{\Gamma} = \begin{bmatrix} \Gamma_{11} & \Gamma_{12} & \Gamma_{13} \\ \Gamma_{21} & \Gamma_{22} & \Gamma_{23} \\ \Gamma_{31} & \Gamma_{32} & \Gamma_{33} \\ \Gamma_{41} & \Gamma_{42} & \Gamma_{43} \end{bmatrix}
= \sum_{k=1}^{N} \begin{bmatrix} \bar{Q}_{11} b_{R_1}^{\mathrm{NL}} & \bar{Q}_{12} e_{R_2}^{\mathrm{NL}} & \bar{Q}_{16} e_{R_1}^{\mathrm{NL}} \\ \bar{Q}_{16} b_{R_1}^{\mathrm{NL}} & \bar{Q}_{26} e_{R_2}^{\mathrm{NL}} & \bar{Q}_{66} e_{R_1}^{\mathrm{NL}} \\ \bar{Q}_{12} e_{R_1}^{\mathrm{NL}} & \bar{Q}_{22} b_{R_2}^{\mathrm{NL}} & \bar{Q}_{26} e_{R_2}^{\mathrm{NL}} \\ \bar{Q}_{16} e_{R_1}^{\mathrm{NL}} & \bar{Q}_{26} b_{R_2}^{\mathrm{NL}} & \bar{Q}_{66} e_{R_2}^{\mathrm{NL}} \end{bmatrix}^{(k)} \tag{31}
$$

$$
\underline{\Delta} = \begin{bmatrix} \Delta_{11} & \Delta_{12} & \Delta_{13} \\ \Delta_{21} & \Delta_{22} & \Delta_{23} \\ \Delta_{31} & \Delta_{32} & \Delta_{33} \\ \Delta_{41} & \Delta_{42} & \Delta_{43} \end{bmatrix}
= \sum_{k=1}^{N} \begin{bmatrix} \bar{Q}_{11} g_{R_1}^{\mathrm{NL}} & \bar{Q}_{12} h_{R_2}^{\mathrm{NL}} & \bar{Q}_{16} h_{R_1}^{\mathrm{NL}} \\ \bar{Q}_{16} g_{R_1}^{\mathrm{NL}} & \bar{Q}_{26} h_{R_2}^{\mathrm{NL}} & \bar{Q}_{66} h_{R_1}^{\mathrm{NL}} \\ \bar{Q}_{12} h_{R_1}^{\mathrm{NL}} & \bar{Q}_{22} g_{R_2}^{\mathrm{NL}} & \bar{Q}_{26} h_{R_2}^{\mathrm{NL}} \\ \bar{Q}_{16} h_{R_1}^{\mathrm{NL}} & \bar{Q}_{26} g_{R_2}^{\mathrm{NL}} & \bar{Q}_{66} h_{R_2}^{\mathrm{NL}} \end{bmatrix}^{(k)} \tag{32}
$$

$$\underline{\mathrm{E}} = \begin{bmatrix} \mathrm{E}_{11} & \mathrm{E}_{12} & \mathrm{E}_{13} & \mathrm{E}_{14} \\ \mathrm{E}_{21} & \mathrm{E}_{22} & \mathrm{E}_{23} & \mathrm{E}_{24} \end{bmatrix} = \sum_{k=1}^{N} \begin{bmatrix} \bar{Q}_{44} a^{\mathrm{NL}}_{R_2} & \bar{Q}_{44} d^{\mathrm{NL}}_{R_2} & \bar{Q}_{45} d^{\mathrm{NL}}_{R_1} & \bar{Q}_{45} d^{\mathrm{NL}}_{R_2} \\ \bar{Q}_{45} d^{\mathrm{NL}}_{R_2} & \bar{Q}_{45} d^{\mathrm{NL}}_{R_1} & \bar{Q}_{55} a^{\mathrm{NL}}_{R_1} & \bar{Q}_{55} d^{\mathrm{NL}}_{R_1} \end{bmatrix}^{(k)} \tag{33}$$

$$\underline{\mathrm{Z}} = \begin{bmatrix} \mathrm{Z}_{11} & \mathrm{Z}_{12} & \mathrm{Z}_{13} & \mathrm{Z}_{14} \\ \mathrm{Z}_{21} & \mathrm{Z}_{22} & \mathrm{Z}_{23} & \mathrm{Z}_{24} \end{bmatrix} = \sum_{k=1}^{N} \begin{bmatrix} \bar{Q}_{44} b^{\mathrm{NL}}_{R_2} & \bar{Q}_{44} e^{\mathrm{NL}}_{R_2} & \bar{Q}_{45} e^{\mathrm{NL}}_{R_1} & \bar{Q}_{45} e^{\mathrm{NL}}_{R_2} \\ \bar{Q}_{45} e^{\mathrm{NL}}_{R_2} & \bar{Q}_{45} e^{\mathrm{NL}}_{R_1} & \bar{Q}_{55} b^{\mathrm{NL}}_{R_1} & \bar{Q}_{55} e^{\mathrm{NL}}_{R_1} \end{bmatrix}^{(k)} \tag{34}$$

$$\underline{\mathrm{H}} = \begin{bmatrix} \mathrm{H}_{11} & \mathrm{H}_{12} & \mathrm{H}_{13} & \mathrm{H}_{14} \\ \mathrm{H}_{21} & \mathrm{H}_{22} & \mathrm{H}_{23} & \mathrm{H}_{24} \end{bmatrix} = \sum_{k=1}^{N} \begin{bmatrix} \bar{Q}_{44} c^{\mathrm{NL}}_{R_2} & \bar{Q}_{44} f^{\mathrm{NL}}_{R_2} & \bar{Q}_{45} f^{\mathrm{NL}}_{R_1} & \bar{Q}_{45} f^{\mathrm{NL}}_{R_2} \\ \bar{Q}_{45} f^{\mathrm{NL}}_{R_2} & \bar{Q}_{45} f^{\mathrm{NL}}_{R_1} & \bar{Q}_{55} c^{\mathrm{NL}}_{R_1} & \bar{Q}_{55} f^{\mathrm{NL}}_{R_1} \end{bmatrix}^{(k)} \tag{35}$$

where

$$\begin{aligned}
a^{\mathrm{NL}}_{R_1} &= \frac{R_1^2}{R_2}\left[\ln\left(\frac{R_1+\zeta_{k+1}}{R_1+\zeta_k}\right) + (R_2-R_1)\frac{(\zeta_{k+1}-\zeta_k)}{(R_1+\zeta_{k+1})(R_1+\zeta_k)}\right] \\
b^{\mathrm{NL}}_{R_1} &= \frac{R_1^2}{R_2}\left[(\zeta_{k+1}-\zeta_k) + (R_2-2R_1)\ln\left(\frac{R_1+\zeta_{k+1}}{R_1+\zeta_k}\right) - R_1(R_2-R_1)\frac{(\zeta_{k+1}-\zeta_k)}{(R_1+\zeta_{k+1})(R_1+\zeta_k)}\right] \\
c^{\mathrm{NL}}_{R_1} &= \frac{R_1^2}{R_2}\left[\frac{1}{2}(\zeta_{k+1}^2-\zeta_k^2) + (R_2-2R_1)(\zeta_{k+1}-\zeta_k) + R_1(3R_1-2R_2)\ln\left(\frac{R_1+\zeta_{k+1}}{R_1+\zeta_k}\right) + R_1^2(R_2-R_1)\frac{(\zeta_{k+1}-\zeta_k)}{(R_1+\zeta_{k+1})(R_1+\zeta_k)}\right] \\
d^{\mathrm{NL}}_{R_1} &= R_1\ln\left(\frac{R_1+\zeta_{k+1}}{R_1+\zeta_k}\right) \\
e^{NL}_{R_1} &= R_1\left[(\zeta_{k+1}-\zeta_k) - R_1\ln\left(\frac{R_1+\zeta_{k+1}}{R_1+\zeta_k}\right)\right] \\
f^{\mathrm{NL}}_{R_1} &= R_1\left[\frac{1}{2}(\zeta_{k+1}^2-\zeta_k^2) - R_1(\zeta_{k+1}-\zeta_k) + R_1^2\ln\left(\frac{R_1+\zeta_{k+1}}{R_1+\zeta_k}\right)\right] \\
g^{\mathrm{NL}}_{R_1} &= \frac{R_1^2}{R_2}\left[\frac{1}{3}(\zeta_{k+1}^3-\zeta_k^3) + \left(\frac{R_2}{2}-R_1\right)(\zeta_{k+1}^2-\zeta_k^2) + R_1(3R_1-2R_2)(\zeta_{k+1}-\zeta_k) + R_1^2(3R_2-4R_1)\ln\left(\frac{R_1+\zeta_{k+1}}{R_1+\zeta_k}\right) - R_1^3(R_2-R_1)\frac{(\zeta_{k+1}-\zeta_k)}{(R_1+\zeta_{k+1})(R_1+\zeta_k)}\right] \\
h^{\mathrm{NL}}_{R_1} &= R_1\left[\frac{1}{3}(\zeta_{k+1}^3-\zeta_k^3) - \frac{1}{2}R_1(\zeta_{k+1}^2-\zeta_k^2) + R_1^2(\zeta_{k+1}-\zeta_k) - R_1^3\ln\left(\frac{R_1+\zeta_{k+1}}{R_1+\zeta_k}\right)\right]
\end{aligned} \tag{36}$$

III. Equations of Motion

The following six equations of equilibrium are widely accepted [2–15]. They reflect the equilibrium of the middle surface when a transverse load q is applied, and they are

$$\begin{aligned}
&\frac{\partial}{\partial\xi_1}(a_2N_{11}) + \frac{\partial}{\partial\xi_2}(a_1N_{21}) - N_{22}\frac{\partial a_2}{\partial\xi_1} + N_{12}\frac{\partial a_1}{\partial\xi_2} + \frac{a_1a_2}{R_1}Q_1 = a_1a_2\left(I_0\frac{\partial^2 u_0}{\partial t^2} + I_1\frac{\partial^2\phi_1}{\partial t^2}\right) \\
&\frac{\partial}{\partial\xi_1}(a_2N_{12}) + \frac{\partial}{\partial\xi_2}(a_1N_{22}) - N_{11}\frac{\partial a_1}{\partial\xi_2} + N_{21}\frac{\partial a_2}{\partial\xi_1} + \frac{a_1a_2}{R_2}Q_2 = a_1a_2\left(I_0\frac{\partial^2 v_0}{\partial t^2} + I_1\frac{\partial^2\phi_2}{\partial t^2}\right) \\
&\frac{\partial}{\partial\xi_1}(a_2Q_1) + \frac{\partial}{\partial\xi_2}(a_1Q_2) - a_1a_2\left(\frac{N_{11}}{R_1} + \frac{N_{22}}{R_2}\right) = qa_1a_2 + a_1a_2I_0\frac{\partial^2 w_0}{\partial t^2} \\
&\frac{\partial}{\partial\xi_1}(a_2M_{11}) + \frac{\partial}{\partial\xi_2}(a_1M_{21}) - M_{22}\frac{\partial a_2}{\partial\xi_1} + M_{12}\frac{\partial a_1}{\partial\xi_2} - a_1a_2Q_1 = a_1a_2\left(I_1\frac{\partial^2 u_0}{\partial t^2} + I_2\frac{\partial^2\phi_1}{\partial t^2}\right) \\
&\frac{\partial}{\partial\xi_1}(a_2M_{12}) + \frac{\partial}{\partial\xi_2}(a_1M_{22}) - M_{11}\frac{\partial a_1}{\partial\xi_2} + M_{21}\frac{\partial a_2}{\partial\xi_1} - a_1a_2Q_2 = a_1a_2\left(I_1\frac{\partial^2 v_0}{\partial t^2} + I_2\frac{\partial^2\phi_2}{\partial t^2}\right) \\
&\frac{M_{21}}{R_2} - \frac{M_{12}}{R_1} + N_{21} - N_{12} = 0
\end{aligned} \tag{37}$$

The mass inertias I_0, I_1, and I_2 are calculated using

$$I_i = \sum_{k=1}^{N}\int_{-h/2}^{h/2}\rho^{(k)}\left(1+\frac{\zeta}{R_1}\right)\left(1+\frac{\zeta}{R_2}\right)\zeta^i\,\mathrm{d}\zeta \qquad (i=0,1,2) \tag{38}$$

where ρ is the mass density.

Because of the definition of the stress resultants, the last expression in Eq. (37), concerning *drilling* equilibrium, is identically satisfied and, for this reason, is usually not considered in deriving the differential equations relating displacements and applied loads. It is noted that drilling equilibrium is always satisfied unless the flat-plate approximation is assumed in the definition of the stress resultants. In fact, in many previous theories in which the term $1+\zeta/R_i$ is approximated to unity, the definition of stress resultants does not satisfy the sixth equilibrium equation.

In deriving the stress resultants, approximate expressions for the displacement field have been used. It has been demonstrated that this discrepancy leads to nonzero strain components (note, not strains) and stress resultants corresponding to a small rigid-body rotation and that Eq. (20) is thus in need of some modification [9,10,13,14]. Analytically, this is done by modifying the strain-displacement relations in Eq. (20) by replacing those terms without tildes using the following terms with tildes:

$$\begin{aligned}
\tilde{\omega}_1^0 &= \frac{1}{a_1}\left(\frac{\partial v_0}{\partial\xi_1} - \frac{u_0}{a_2}\frac{\partial a_1}{\partial\xi_2}\right) - \phi_n \\
\tilde{\omega}_2^0 &= \frac{1}{a_2}\left(\frac{\partial u_0}{\partial\xi_2} - \frac{v_0}{a_1}\frac{\partial a_2}{\partial\xi_1}\right) + \phi_n \\
\tilde{\omega}_1^1 &= \frac{1}{a_1}\left(\frac{\partial\phi_2}{\partial\xi_1} - \frac{\phi_1}{a_2}\frac{\partial a_1}{\partial\xi_2}\right) - \frac{\phi_n}{R_1} \\
\tilde{\omega}_2^1 &= \frac{1}{a_2}\left(\frac{\partial\phi_1}{\partial\xi_2} - \frac{\phi_2}{a_1}\frac{\partial a_2}{\partial\xi_1}\right) + \frac{\phi_n}{R_2}
\end{aligned} \tag{39}$$

Here, the term ϕ_n is the third component of the curl of the shell's middle-surface displacement field; hence,

$$\phi_n = \frac{1}{2a_1a_2}\left[\frac{\partial}{\partial\xi_1}(a_2v_0) - \frac{\partial}{\partial\xi_2}(a_1u_0)\right] \tag{40}$$

The same correction does not apply to Eqs. (26–28). This reasoning is understood by considering the work of Sanders [13], in which he imposed the displacement field, generated by a small rigid rotation, on the structure. Because he was dealing with a linear theory and small displacements, he could approximate the small rigid rotation with a curl. In linear theories, this must result in zero strain components, and thus the correction. In nonlinear theories, a curl cannot be approximated to a rigid rotation. It actually entails some deformations, and these deformations are analytically described by the nonlinear strains in Eq. (16). The physical meaning of the latter equation would be altered by applying the curl correction to Eqs. (26–28).

IV. Numerical Results

One of the features on the present work is that the term $1 + \zeta/R_i$ has been retained in the derivation of the shell model. This term is typically neglected because, for the range of applicability of any shell theory based on an approximation of the shell as a two-dimensional structure, the quantity ζ/R_i is small if compared with unity.

In the following sections, examples of application of the developed theory are presented. The expressions of the stiffnesses are presented as functions of the geometry of the shell in its orthogonal conjugate curvilinear system (i.e., of the normal radii of curvature). These functions therefore represent a point-to-point mapping between the structure's idealized domain and stiffness. In other words, they allow one to analytically calculate the exact stiffnesses of a differential element within a structure.

It is later shown that even when the approximation $\zeta/R_i \ll 1$ holds correctly, neglecting this term entails the loss of important information. Indeed, the geometry of a shell structure can affect the stiffness matrix by introducing coupling terms for even symmetric laminates or isotropic materials. This effect is readily explained by simplifying the expressions in Eq. (25). For instance, consider a generic shell of thickness h and assume that the material is isotropic. A series expansion of Eqs. (25) yields the following relationships:

$$a^L_{R_1} \approx a^L_{R_2} \approx h - \frac{1}{12}\frac{h^3}{R_1}\left(\frac{1}{R_2} - \frac{1}{R_1}\right)$$
$$b^L_{R_1} \approx b^L_{R_2} \approx \frac{h^3}{12}\left(\frac{1}{R_2} - \frac{1}{R_1}\right), \qquad e^L_{R_1} \approx \frac{1}{12}h^3 \tag{41}$$
$$e^L_{R_2} \approx \frac{1}{12}h^3 + \frac{1}{80}\frac{h^5}{R_2}\left(\frac{1}{R_2} - \frac{1}{R_1}\right)$$

Equations (41) give an idea of the order of magnitude of the difference between classic lamination theory stiffnesses and those herein presented, and they also show that this difference depends on thickness, radii of curvature. and the sign of their product R_1R_2. By comparing the latter expressions with the classic case (P.A.) in which

$$a^L_{R_1} \approx a^L_{R_2} \approx h, \qquad b^L_{R_1} \approx b^L_{R_2} \approx 0, \qquad e^L_{R_1} \approx e^L_{R_2} \approx \tfrac{1}{12}h^3 \tag{42}$$

it becomes clear that, with the notable exception of the sphere, there is a small nonuniform relative difference for the A_{ij} and D_{ij} terms and that the same difference, which is magnified for structures in which $R_1R_2 < 0$, is larger in B_{ij} terms. Indeed, the latter differ from zero by the order of D_{ij}/R_i. For composite structures, these differences are then expected to be of the same order of magnitude as those obtained using Eqs. (41) and (42).

The bending-stretching matrix is nonzero, even for symmetrically laminated structures, due to the inherent geometry. An important general rule may be deduced from the expressions in Eqs. (41): that is, the effect of the initial geometry on the elastic behavior of a curved surface depends on its Gaussian curvature (GC). This quantity is defined as the product of the principal curvatures and it is positive for synclastic surfaces (e.g., elliptic paraboloids), zero for developable or ruled surfaces (e.g., cylinders or cones) and negative for anticlastic surfaces (e.g., hyperbolic paraboloids). For structures with different geometries and identical thicknesses and lamination, the magnitude of the elements of the bending-stretching matrix increases for decreasing GC. In summary, from Eq. (41),

$$\mathrm{GC} > 0 \Rightarrow B_{ij} \cong \mathcal{O}\left(\frac{h^3}{|R_2|} - \frac{h^3}{|R_1|}\right)$$
$$\mathrm{GC} = 0 \Rightarrow B_{ij} \cong \mathcal{O}\left(\frac{h^3}{|R_2|}\right) \tag{43}$$
$$\mathrm{GC} < 0 \Rightarrow B_{ij} \cong \mathcal{O}\left(\frac{h^3}{|R_2|} + \frac{h^3}{|R_1|}\right)$$

.

Interestingly, the significance of the B_{ij} terms depends only on geometry, via GC, and not on material stiffness properties. As such, the effect of curvature on B_{ij} is completely captured by GC, noting that the largest effects occur for anticlastic geometries, such as the hyperbolic paraboloid (negative GC), and the smallest effects occur for synclastic curvatures (positive GC), with zero effect for spheres. Curvature effects on B_{ij} for cylindrical shells are intermediate between the two previous examples, as may be expected, due to their zero GC value.

In the following sections, stiffness matrices resulting from Eqs. (21–24) are compared with the equivalent P.A. matrices, as in [10]. Results for synclastic, developable, and anticlastic surfaces are shown with the aim of showing both the order of magnitude of the difference and the relationship between the difference and the Gaussian curvature.

The material properties used in the following examples are $E_1 = 206.8$ GPa, $E_2 = 20.7$ GPa, $\nu_{12} = 0.25$, $G_{12} = G_{13} =$ 10.3 GPa, and $G_{23} = 4.1$ GPa. Two different layups with stacking sequences $[45 \quad 30 \quad 90 \quad 0]_S$ and $[90_4 \quad 0_4]_T$ are considered. All of the structures have been chosen to have thickness $h = 0.01$ m and thickness-to-radius ratios equal to 0.1 and less than 0.1, respectively.

For a useful comparison note that literature for shells having the aforementioned features considers $N_{12} = N_{21}$, $M_{12} = M_{21}$,

$$\begin{Bmatrix} N_{11} \\ N_{22} \\ N_{12} \end{Bmatrix} = \begin{bmatrix} A_{11} & A_{12} & A_{16} \\ A_{12} & A_{22} & A_{26} \\ A_{16} & A_{26} & A_{66} \end{bmatrix} \begin{Bmatrix} e^0_1 \\ e^0_2 \\ \omega^0_1 + \omega^0_2 \end{Bmatrix} + \begin{bmatrix} B_{11} & B_{12} & B_{16} \\ B_{12} & B_{22} & B_{26} \\ B_{16} & B_{26} & B_{66} \end{bmatrix} \begin{Bmatrix} e^1_1 \\ e^1_2 \\ \omega^1_1 + \omega^1_2 \end{Bmatrix} \tag{44}$$

and

$$\begin{Bmatrix} M_{11} \\ M_{22} \\ M_{12} \end{Bmatrix} = \begin{bmatrix} B_{11} & B_{12} & B_{16} \\ B_{12} & B_{22} & B_{26} \\ B_{16} & B_{26} & B_{66} \end{bmatrix} \begin{Bmatrix} e^0_1 \\ e^0_2 \\ \omega^0_1 + \omega^0_2 \end{Bmatrix} + \begin{bmatrix} D_{11} & D_{12} & D_{16} \\ D_{12} & D_{22} & D_{26} \\ D_{16} & D_{26} & D_{66} \end{bmatrix} \begin{Bmatrix} e^1_1 \\ e^1_2 \\ \omega^1_1 + \omega^1_2 \end{Bmatrix} \tag{45}$$

In the following, a series of tables shows a comparison between stiffness coefficients multiplying the same component of strain.

A. Elliptic Paraboloid

In Tables 1–6, the stiffness coefficients of an elliptic paraboloid are presented. They correspond to the point on the top of the structure that has been defined to have $R_1 = 1/10$ m and $R_2 = 1/15$ m.

Notably, the following relationships hold:

$$\underline{B}^{AE}(R_1, R_2) = \begin{bmatrix} B_{11} & B'_{16} & 0 & 0 \\ B'_{16} & B'_{66} & 0 & 0 \\ 0 & 0 & B_{22} & B''_{26} \\ 0 & 0 & B''_{26} & B''_{66} \end{bmatrix}$$
$$\underline{B}^{PA} = \begin{bmatrix} B_{11} & B_{12} & B_{16} \\ B_{12} & B_{22} & B_{26} \\ B_{16} & B_{26} & B_{66} \end{bmatrix} = \begin{bmatrix} 0 & 0 & 0 \\ 0 & 0 & 0 \\ 0 & 0 & 0 \end{bmatrix} \tag{46}$$

Table 1 Stiffness A_{ij} parameters for $[45\quad 30\quad 90\quad 0]_S$ laminated elliptic paraboloid at its peak

	Plate approximation	Present equations			
(i, j)	A_{ij}, GN/m	A_{ij}, GN/m	A'_{ij}, GN/m	A''_{ij}, GN/m	Error %
(1, 1)	1.0681	1.0683	N/A	N/A	0.02
(2, 2)	0.8339	0.8338	N/A	N/A	−0.01
(1, 6)	0.2664	N/A	0.2666	N/A	0.08
(6, 6)	0.2972	N/A	0.2973	N/A	0.03
(2, 6)	0.1705	N/A	N/A	0.1705	<0.01
(6, 6)	0.2972	N/A	N/A	0.2972	<0.01
(4, 4)	0.0685	0.0685	N/A	N/A	<0.01
(5, 5)	0.0763	0.0763	N/A	N/A	<0.01

Table 2 Stiffness B_{ij} parameters for $[45\quad 30\quad 90\quad 0]_S$ laminated elliptic paraboloid at its peak

	Plate approximation	Present equations			
(i, j)	$10^{-5} \cdot B_{ij}$, GN	$10^{-5} \cdot B_{ij}$, GN	$10^{-5} \cdot B'_{ij}$, GN	$10^{-5} \cdot B''_{ij}$, GN	Error %
(1, 1)	0.00	−2.3373	N/A	N/A	N/A
(2, 2)	0.00	2.0690	N/A	N/A	N/A
(1, 6)	0.00	N/A	−1.2462	N/A	N/A
(6, 6)	0.00	N/A	−1.2744	N/A	N/A
(2, 6)	0.00	N/A	N/A	0.9299	N/A
(6, 6)	0.00	N/A	N/A	1.2746	N/A

Table 3 Stiffness D_{ij} parameters for $[45\quad 30\quad 90\quad 0]_S$ laminated elliptic paraboloid at its peak

	Plate approximation	Present equations			
(i, j)	$10^{-6} \cdot D_{ij}$, GN · m	$10^{-6} \cdot D_{ij}$, GN · m	$10^{-6} \cdot D'_{ij}$, GN · m	$10^{-6} \cdot D''_{ij}$, GN · m	Error %
(1, 1)	7.0109	7.0112	N/A	N/A	<0.01
(2, 2)	6.1571	6.1322	N/A	N/A	−0.40
(1, 6)	3.7342	N/A	3.7357	N/A	0.04
(6, 6)	3.8178	N/A	3.8195	N/A	0.04
(2, 6)	2.7851	N/A	N/A	2.7828	−0.08
(6, 6)	3.8178	N/A	N/A	3.8147	−0.08

Table 4 Stiffness A_{ij} parameters for $[90_4\quad 0_4]_T$ laminated elliptic paraboloid at its peak

	Plate approximation	Present equations			
(i, j)	A_{ij}, GN/m	A_{ij}, GN/m	A'_{ij}, GN/m	A''_{ij}, GN/m	Error %
(1, 1)	1.1448	1.1373	N/A	N/A	−0.66
(2, 2)	1.1448	1.1368	N/A	N/A	−0.70
(1, 6)	0.00	N/A	0.00	N/A	0.00
(6, 6)	0.1034	N/A	0.1035	N/A	0.10
(2, 6)	0.00	N/A	N/A	0.00	0.00
(6, 6)	0.1034	N/A	N/A	0.1034	<0.01
(4, 4)	0.0724	0.0721	N/A	N/A	−0.41
(5, 5)	0.0724	0.0722	N/A	N/A	−0.28

Table 5 Stiffness B_{ij} parameters for $[90_4\quad 0_4]_T$ laminated elliptic paraboloid at its top

	Plate approximation	Present equations			
(i, j)	$10^{-3} \cdot B_{ij}$, GN	$10^{-3} \cdot B_{ij}$, GN	$10^{-3} \cdot B'_{ij}$, GN	$10^{-3} \cdot B''_{ij}$, GN	Error %
(1, 1)	2.3416	2.3107	N/A	N/A	−1.32
(2, 2)	−2.3416	−2.3090	N/A	N/A	−1.39
(1, 6)	0.00	N/A	0.00	N/A	0.00
(6, 6)	0.00	N/A	−0.0028	N/A	N/A
(2, 6)	0.00	N/A	N/A	0.00	0.00
(6, 6)	0.00	N/A	N/A	0.0028	N/A

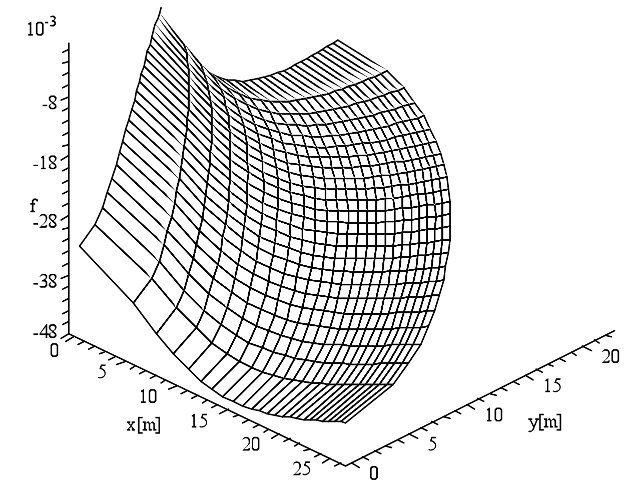

Fig. 1 Trend of $h(1/R_2 - 1/R_1)$ over a quarter of elliptic paraboloid.

As expected, the difference between the new and classic B_{ij} elements in Eqs. (46) is of the order of D_{ij}/R_i and, as shown by the $b^L_{R_i}$ terms in Eq. (37), is proportional to $h(1/R_2 - 1/R_1)$. Because of this proportionality, the coupling follows the trend shown in Fig. 1. It is also interesting to highlight that the effects of the curvature on the stiffness matrices are remarkably larger for the unsymmetric layup. These effects are also observed in the following examples concerning a cylinder and a hyperbolic paraboloid and appear to be a general feature.

B. Cylindrical Shell

Tables 7–12 refer to a cylindrical structure. The radii of curvature are constant through the domain so that $1/R_2 = 10\ \mathrm{m}^{-1}$ and $1/R_1 = 0\ \mathrm{m}^{-1}$. The relationship between the stiffnesses and Gaussian curvature is clearly shown in Tables 1–18. The errors are indeed progressively larger as GC decreases. As already mentioned, this feature is magnified for unsymmetric stacking sequences.

C. Hyperbolic Paraboloid

In Tables 13–18, the stiffness coefficients of a hyperbolic paraboloid are presented. They correspond to the saddle point of the structure that has been taken to have $1/R_1 = -10\ \mathrm{m}^{-1}$ and $1/R_2 = 10\ \mathrm{m}^{-1}$. The distribution of B_{ij} terms follows the trend shown in Fig. 2 and shows significant values, with their maximum occurring at the center of the structure.

V. Geometrically Exact Strain Components

Tables 19–28 show a comparison between the components of strain obtained using the present formulation [present equations (P.E.)] and those valid for plates and commonly used for shells (P.A.). The effect of accurately calculated stiffness coefficients on free vibrations has been investigated in [4]. The main focus here is to show that the same approach may have relevant influences on the nonlinear behavior of shell structures. In fact, it is shown that even the slightest difference in the stiffness matrix may lead to appreciably different components of strain. This is shown by applying unitary stress resultants to the structural points of the symmetric laminate,

Table 6 Stiffness D_{ij} parameters for $[\,90_4\quad 0_4\,]_T$ laminated elliptic paraboloid at its top

	Plate approximation	Present equations			
(i,j)	$10^{-6}\cdot D_{ij}$, GN · m	$10^{-6}\cdot D_{ij}$, GN · m	$10^{-6}\cdot D'_{ij}$, GN · m	$10^{-6}\cdot D''_{ij}$, GN · m	Error %
(1, 1)	9.5399	9.4470	N/A	N/A	−0.97
(2, 2)	9.5399	9.4167	N/A	N/A	−1.29
(1, 6)	0.00	N/A	0.00	N/A	0.00
(6, 6)	0.8618	N/A	0.8621	N/A	0.03
(2, 6)	0.00	N/A	N/A	0.00	0.00
(6, 6)	0.8618	N/A	N/A	0.8604	−0.16

Table 7 Stiffness A_{ij} parameters for $[\,45\quad 30\quad 90\quad 0\,]_S$ laminated cylinder ($1/R = 0.1$)

	Plate approximation	Present equations			
(i,j)	A_{ij}, GN/m	A_{ij}, GN/m	A'_{ij}, GN/m	A''_{ij}, GN/m	Error %
(1, 1)	1.0681	1.0681	N/A	N/A	0.00
(2, 2)	0.8339	0.8345	N/A	N/A	0.07
(1, 6)	0.2664	N/A	0.2664	N/A	0.00
(6, 6)	0.2972	N/A	0.2972	N/A	0.00
(2, 6)	0.1705	N/A	N/A	0.1708	0.18
(6, 6)	0.2972	N/A	N/A	0.2976	0.13
(4, 4)	0.0685	0.0686	N/A	N/A	0.15
(5, 5)	0.0763	0.0763	N/A	N/A	0.00

Table 8 Stiffness B_{ij} parameters for $[\,45\quad 30\quad 90\quad 0\,]_S$ laminated cylinder ($1/R = 0.1$)

	Plate approximation	Present equations			
(i,j)	$10^{-5}\cdot B_{ij}$, GN	$10^{-5}\cdot B_{ij}$, GN	$10^{-5}\cdot B'_{ij}$, GN	$10^{-5}\cdot B''_{ij}$, GN	Error %
(1, 1)	0.00	7.0109	N/A	N/A	N/A
(2, 2)	0.00	−6.1655	N/A	N/A	N/A
(1, 6)	0.00	N/A	3.7342	N/A	N/A
(6, 6)	0.00	N/A	3.8178	N/A	N/A
(2, 6)	0.00	N/A	N/A	−2.7901	N/A
(6, 6)	0.00	N/A	N/A	−3.8241	N/A

Table 9 Stiffness D_{ij} parameters for [45 30 90 0]$_S$ laminated cylinder ($1/R = 0.1$)

	Plate approximation	Present equations			
(i, j)	$10^{-6} \cdot D_{ij}$, GN · m	$10^{-6} \cdot D_{ij}$, GN · m	$10^{-6} \cdot D'_{ij}$, GN · m	$10^{-6} \cdot D''_{ij}$, GN · m	Error %
(1, 1)	7.0109	7.0109	N/A	N/A	0.00
(2, 2)	6.1571	6.1655	N/A	N/A	0.14
(1, 6)	3.7342	N/A	3.7342	N/A	0.00
(6, 6)	3.8178	N/A	3.8178	N/A	0.00
(2, 6)	2.7851	N/A	N/A	2.7901	0.18
(6, 6)	3.8178	N/A	N/A	3.8241	0.17

Table 10 Stiffness A_{ij} parameters for [90_4 0_4]$_T$ laminated cylinder ($1/R = 0.1$)

	Plate approximation	Present equations			
(i, j)	A_{ij}, GN/m	A_{ij}, GN/m	A'_{ij}, GN/m	A''_{ij}, GN/m	Error %
(1, 1)	1.1448	1.1682	N/A	N/A	2.04
(2, 2)	1.1448	1.1692	N/A	N/A	2.13
(1, 6)	0.00	N/A	0.00	N/A	0.00
(6, 6)	0.1034	N/A	0.1034	N/A	0.00
(2, 6)	0.00	N/A	N/A	0.00	0.00
(6, 6)	0.1034	N/A	N/A	0.1035	0.10
(4, 4)	0.0724	0.0732	N/A	N/A	1.10
(5, 5)	0.0724	0.0732	N/A	N/A	1.10

Table 11 Stiffness B_{ij} parameters for [90_4 0_4]$_T$ laminated cylinder ($1/R = 0.1$)

	Plate approximation	Present equations			
(i, j)	$10^{-3} \cdot B_{ij}$, GN	$10^{-3} \cdot B_{ij}$, GN	$10^{-3} \cdot B'_{ij}$, GN	$10^{-3} \cdot B''_{ij}$, GN	Error %
(1, 1)	2.3416	2.4370	N/A	N/A	4.07
(2, 2)	−2.3416	−2.4401	N/A	N/A	4.21
(1, 6)	0.00	N/A	0.00	N/A	0.00
(6, 6)	0.00	N/A	0.0086	N/A	N/A
(2, 6)	0.00	N/A	N/A	0.00	0.00
(6, 6)	0.00	N/A	N/A	−0.0086	N/A

Table 12 Stiffness D_{ij} parameters for [90_4 0_4]$_T$ laminated cylinder ($1/R = 0.1$)

	Plate approximation	Present equations			
(i, j)	$10^{-6} \cdot D_{ij}$, GN · m	$10^{-6} \cdot D_{ij}$, GN · m	$10^{-6} \cdot D'_{ij}$, GN · m	$10^{-6} \cdot D''_{ij}$, GN · m	Error %
(1, 1)	9.5399	9.8326	N/A	N/A	3.07
(2, 2)	9.5399	9.8474	N/A	N/A	3.22
(1, 6)	0.00	N/A	0.00	N/A	0.00
(6, 6)	0.8618	N/A	0.8618	N/A	0.00
(2, 6)	0.00	N/A	N/A	0.00	0.00
(6, 6)	0.8618	N/A	N/A	0.8631	0.15

Table 13 Stiffness A_{ij} parameters for [45 30 90 0]$_S$ laminated hyperbolic paraboloid at its saddle point

	Plate approximation	Present equations			
(i, j)	A_{ij}, GN/m	A_{ij}, GN/m	A'_{ij}, GN/m	A''_{ij}, GN/m	Error %
(1, 1)	1.0681	1.0695	N/A	N/A	0.13
(2, 2)	0.8339	0.8351	N/A	N/A	0.14
(1, 6)	0.2664	N/A	0.2672	N/A	0.30
(6, 6)	0.2972	N/A	0.2980	N/A	0.27
(2, 6)	0.1705	N/A	N/A	0.1711	0.35
(6, 6)	0.2972	N/A	N/A	0.2980	0.27
(4, 4)	0.0685	0.0686	N/A	N/A	0.15
(5, 5)	0.0763	0.0764	N/A	N/A	0.13

Table 14 Stiffness B_{ij} parameters for $[45 \quad 30 \quad 90 \quad 0]_S$ laminated hyperbolic paraboloid at its saddle point

	Plate approximation	Present equations			
(i, j)	$10^{-4} \cdot B_{ij}$, GN	$10^{-4} \cdot B_{ij}$, GN	$10^{-4} \cdot B'_{ij}$, GN	$10^{-4} \cdot B''_{ij}$, GN	Error %
(1, 1)	0.00	1.4043	N/A	N/A	N/A
(2, 2)	0.00	−1.2334	N/A	N/A	N/A
(1, 6)	0.00	N/A	0.7480	N/A	N/A
(6, 6)	0.00	N/A	0.7648	N/A	N/A
(2, 6)	0.00	N/A	N/A	−0.5580	N/A
(6, 6)	0.00	N/A	N/A	−0.7647	N/A

Table 15 Stiffness D_{ij} parameters for $[45 \quad 30 \quad 90 \quad 0]_S$ laminated hyperbolic paraboloid at its saddle point

	Plate approximation	Present equations			
(i, j)	$10^{-6} \cdot D_{ij}$, GN · m	$10^{-6} \cdot D_{ij}$, GN · m	$10^{-6} \cdot D'_{ij}$, GN · m	$10^{-6} \cdot D''_{ij}$, GN · m	Error %
(1, 1)	7.0109	7.0315	N/A	N/A	0.29
(2, 2)	6.1571	6.1771	N/A	N/A	0.32
(1, 6)	3.7342	N/A	3.7456	N/A	0.31
(6, 6)	3.8178	N/A	3.8302	N/A	0.32
(2, 6)	2.7851	N/A	N/A	2.7952	0.36
(6, 6)	3.8178	N/A	N/A	3.8291	0.30

Table 16 Stiffness A_{ij} parameters for $[90_4 \quad 0_4]_T$ laminated hyperbolic paraboloid at its saddle point

	Plate approximation	Present equations			
(i, j)	A_{ij}, GN/m	A_{ij}, GN/m	A'_{ij}, GN/m	A''_{ij}, GN/m	Error %
(1, 1)	1.1448	1.1936	N/A	N/A	4.26
(2, 2)	1.1448	1.1936	N/A	N/A	4.26
(1, 6)	0.00	N/A	0.00	N/A	0.00
(6, 6)	0.1034	N/A	0.1036	N/A	0.19
(2, 6)	0.00	N/A	N/A	0.00	0.00
(6, 6)	0.1034	N/A	N/A	0.1036	0.19
(4, 4)	0.0724	0.0741	N/A	N/A	2.35
(5, 5)	0.0724	0.0741	N/A	N/A	2.35

Table 17 Stiffness B_{ij} parameters for $[90_4 \quad 0_4]_T$ laminated hyperbolic paraboloid at its saddle point

	Plate approximation	Present equations			
(i, j)	$10^{-3} \cdot B_{ij}$, GN	$10^{-3} \cdot B_{ij}$, GN	$10^{-3} \cdot B'_{ij}$, GN	$10^{-3} \cdot B''_{ij}$, GN	Error %
(1, 1)	2.3416	2.5386	N/A	N/A	8.41
(2, 2)	−2.3416	−2.5386	N/A	N/A	8.41
(1, 6)	0.00	N/A	0.00	N/A	0.00
(6, 6)	0.00	N/A	0.0172	N/A	N/A
(2, 6)	0.00	N/A	N/A	0.00	0.00
(6, 6)	0.00	N/A	N/A	−0.0172	N/A

Table 18 Stiffness D_{ij} parameters for $[90_4 \quad 0_4]_T$ laminated hyperbolic paraboloid at its saddle point

	Plate approximation	Present equations			
(i, j)	$10^{-6} \cdot D_{ij}$, GN · m	$10^{-6} \cdot D_{ij}$, GN · m	$10^{-6} \cdot D'_{ij}$, GN · m	$10^{-6} \cdot D''_{ij}$, GN · m	Error %
(1, 1)	9.5399	10.1560	N/A	N/A	6.46
(2, 2)	9.5399	10.1381	N/A	N/A	6.27
(1, 6)	0.00	N/A	0.00	N/A	0.00
(6, 6)	0.8618	N/A	0.8645	N/A	0.31
(2, 6)	0.00	N/A	N/A	0.00	0.00
(6, 6)	0.8618	N/A	N/A	0.8638	0.23

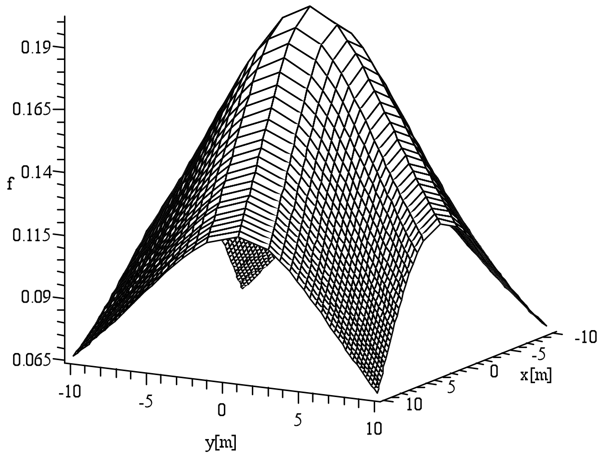

Fig. 2 Trend of $h(1/R_2 - 1/R_1)$ over a hyperbolic paraboloid.

used in the previous sections, and calculating the resulting deformations by inverting Eq. (20).

Data in Tables 25 and 26 include effects of combined stretching-bending. The large discrepancies are explained in terms of orders of magnitude effects by using the same assumptions that led to Eqs. (41) and (42). The following expressions are obtained by inverting Eq. (20) and applying loads as in Tables 25 and 26. In fact, one can show that the errors are proportional to

$$\frac{(1/R_2)-(1/R_1)}{\{1-(h^2/12)[(1/R_2)-(1/R_1)]^2\}}\left[\frac{h^2}{12}\left(\frac{1}{R_2}-\frac{1}{R_1}\right)-1\right] \cong \mathcal{O}(10^3)\% \tag{47}$$

and

$$\frac{(h^2/12)[(1/R_2)-(1/R_1)]}{\{1-(h^2/12)[(1/R_2)-(1/R_1)]^2\}}\left[\left(\frac{1}{R_2}-\frac{1}{R_1}\right)-1\right] \cong \mathcal{O}(10^{-2})\% \tag{48}$$

for in-plane and out-of-plane components of deformation, respectively. The order of magnitude of the error for the in-plane components of strain is thus explained. It is due to the presence of a populated coupling matrix and obviously tends to zero when the principal curvatures tend to infinity.

The data in Table 28 are particularly interesting because they present a loading condition that cannot be reproduced by assuming the plate approximation. In that case, the artificially achieved

Table 19 Strain components for $[45\ \ 30\ \ 90\ \ 0]_S$ laminate

	Applied load $N_{11} = 1$ N/m, $Q_{11} = 1$ N/m						
		Paraboloid		Cylinder		Hyperboloid	
	$10^{-9}\cdot$ P.A.	$10^{-9}\cdot$ P.E.	Error %	$10^{-9}\cdot$ P.E.	Error %	$10^{-9}\cdot$ P.E.	Error %
e_1^0	1.2232	1.229	0.47	1.2297	0.53	1.2302	0.57
e_2^0	−0.1545	−0.1387	−10.21	−0.1386	−10.26	−0.1385	−10.35
$\omega_1^0+\omega_2^0$	−1.0079	−0.7595	−24.65	−0.7595	−24.64	−0.7596	−24.63
e_4^0	−2.8853	−2.885	−0.01	−2.8827	−0.09	−2.8753	−0.35
e_5^0	13.6583	13.6545	−0.03	13.6578	<0.01	13.6343	−0.18
e_1^1	0	4.3098	N/A	−12.381	N/A	−24.9202	N/A
e_2^1	0	−0.3541	N/A	0.426	N/A	1.0613	N/A
$\omega_1^1+\omega_2^1$	0	−4.6293	N/A	3.5694	N/A	10.5564	N/A

Table 20 Strain components for $[45\ \ 30\ \ 90\ \ 0]_S$ laminate

	Applied load $N_{22} = 1$ N/m, $Q_{22} = 1$ N/m						
		Paraboloid		Cylinder		Hyperboloid	
	$10^{-9}\cdot$ P.A.	$10^{-9}\cdot$ P.E.	Error %	$10^{-9}\cdot$ P.E.	Error %	$10^{-9}\cdot$ P.E.	Error %
e_1^0	−0.1545	−0.1387	−10.21	−0.1386	−10.26	−0.1385	−10.35
e_2^0	1.3781	1.4204	3.07	1.4202	3.05	1.4218	3.17
$\omega_1^0+\omega_2^0$	−0.6522	0.0101	−101.55	0.0103	−101.59	0.0098	−101.5
e_4^0	15.2045	15.2074	0.02	15.1909	−0.09	15.1762	−0.19
e_5^0	−2.8853	−2.885	−0.01	−2.8827	−0.09	−2.8753	−0.35
e_1^1	0	0.9414	N/A	−1.375	N/A	−3.2243	N/A
e_2^1	0	−5.2142	N/A	13.9371	N/A	28.4382	N/A
$\omega_1^1+\omega_2^1$	0	−6.6581	N/A	−7.5181	N/A	−5.8672	N/A

Table 21 Strain components for $[45\ \ 30\ \ 90\ \ 0]_S$ laminate

	Applied load $N_{11} = 1$ N/m, $N_{22} = 1$ N/m						
		Paraboloid		Cylinder		Hyperboloid	
	$10^{-9}\cdot$ P.A.	$10^{-9}\cdot$ P.E.	Error %	$10^{-9}\cdot$ P.E.	Error %	$10^{-9}\cdot$ P.E.	Error %
e_1^0	1.0687	1.0903	2.02	1.091	2.09	1.0917	2.15
e_2^0	1.2236	1.2817	4.75	1.2815	4.74	1.2833	4.88
$\omega_1^0+\omega_2^0$	−1.66	−0.7494	−54.86	−0.7492	−54.87	−0.7498	−54.83
e_1^1	0	5.2512	N/A	−13.7561	N/A	−28.1445	N/A
e_2^1	0	−5.5683	N/A	14.3632	N/A	29.4995	N/A
$\omega_1^1+\omega_2^1$	0	−11.2873	N/A	−3.9488	N/A	4.6892	N/A

Table 22 Strain components for [45 30 90 0]$_S$ laminate

	Applied load $M_{11} = 1$ N						
		Paraboloid		Cylinder		Hyperboloid	
	$10^{-6}\cdot$ P.A.	$10^{-6}\cdot$ P.E.	Error %	$10^{-6}\cdot$ P.E.	Error %	$10^{-6}\cdot$ P.E.	Error %
e_1^0	0	0.0043	N/A	−0.0124	N/A	−0.0249	N/A
e_2^0	0	0.0009	N/A	−0.0014	N/A	−0.0032	N/A
$\omega_1^0+\omega_2^0$	0	0.0045	N/A	0.0094	N/A	0.0112	N/A
e_1^1	307.5838	307.467	−0.04	307.7032	0.04	307.2542	−0.11
e_2^1	−49.6147	−49.615	<0.01	−49.5925	−0.04	−49.5103	−0.21
$\omega_1^1+\omega_2^1$	−264.6526	−264.6258	−0.01	−264.7113	0.02	−264.163	−0.18

Table 23 Strain components for [45 30 90 0]$_S$ laminate

	Applied load $M_{22} = 1$ N						
		Paraboloid		Cylinder		Hyperboloid	
	$10^{-6}\cdot$ P.A.	$10^{-6}\cdot$ P.E.	Error %	$10^{-6}\cdot$ P.E.	Error %	$10^{-6}\cdot$ P.E.	Error %
e_1^0	0	−0.0004	N/A	0.0004	N/A	0.0011	N/A
e_2^0	0	−0.0052	N/A	0.0139	N/A	0.0284	N/A
$\omega_1^0+\omega_2^0$	0	−0.0059	N/A	−0.0091	N/A	−0.0092	N/A
e_1^1	−49.6147	−49.615	<0.01	−49.5925	−0.04	−49.5103	−0.21
e_2^1	250.4062	250.4879	0.03	250.2728	−0.05	250.4132	<0.01
$\omega_1^1+\omega_2^1$	−134.1468	−134.0989	−0.04	−134.03	−0.9	−134.0839	−0.05

Table 24 Strain components for [45 30 90 0]$_S$ laminate

	Applied load $M_{11} = 1$ N, $M_{22} = 1$ N						
		Paraboloid		Cylinder		Hyperboloid	
	$10^{-6}\cdot$ P.A.	$10^{-6}\cdot$ P.E.	Error %	$10^{-6}\cdot$ P.E.	Error %	$10^{-6}\cdot$ P.E.	Error %
e_1^0	0	0.004	N/A	−0.012	N/A	−0.0239	N/A
e_2^0	0	−0.0043	N/A	0.0126	N/A	0.0252	N/A
$\omega_1^0+\omega_2^0$	0	−0.0014	N/A	0.0003	N/A	0.0019	N/A
e_1^1	257.9691	257.852	−0.05	258.1106	0.05	257.7439	−0.09
e_2^1	200.7915	200.8729	0.04	200.6803	−0.06	200.9029	0.06
$\omega_1^1+\omega_2^1$	−398.7993	−398.7246	−0.02	−398.7413	−0.01	−398.2469	−0.14

Table 25 Strain components for [45 30 90 0]$_S$ laminate

	Applied load $N_{11} = 1$ N/m, $M_{11} = 1$ N						
		Paraboloid		Cylinder		Hyperboloid	
	$10^{-6}\cdot$ P.A.	$10^{-6}\cdot$ P.E.	Error %	$10^{-6}\cdot$ P.E.	Error %	$10^{-6}\cdot$ P.E.	Error %
e_1^0	0.0012	0.0055	352.8	−0.0112	−1011.63	−0.0237	−2036.67
e_2^0	−0.0002	0.0008	−619.53	−0.0015	879.75	−0.0034	2076.64
$\omega_1^0+\omega_2^0$	−0.001	0.0037	−468.14	0.0086	−956.33	0.0104	−1132.13
e_1^1	307.5838	307.4713	−0.04	307.6908	0.03	307.2293	−0.12
e_2^1	−49.6147	−49.6153	<0.01	−49.5921	−0.05	−49.5092	−0.21
$\omega_1^1+\omega_2^1$	−264.6526	−264.6304	−0.01	−264.7078	0.02	−264.1524	−0.19

Table 26 Strain components for [45 30 90 0]$_S$ laminate

	Applied load $N_{22} = 1$ N/m, $M_{22} = 1$ N						
		Paraboloid		Cylinder		Hyperboloid	
	$10^{-6}\cdot$ P.A.	$10^{-6}\cdot$ P.E.	Error %	$10^{-6}\cdot$ P.E.	Error %	$10^{-6}\cdot$ P.E.	Error %
e_1^0	−0.0002	−0.0005	219.01	0.0003	−286.02	0.0009	−697.31
e_2^0	0.0014	−0.0038	−375.3	0.0154	1014.41	0.0299	2066.81
$\omega_1^0+\omega_2^0$	−0.0007	−0.0058	796.08	−0.009	1287.63	−0.0092	1315.73
e_1^1	−49.6147	−49.614	<0.01	−49.5939	−0.04	−49.5135	−0.2
e_2^1	250.4062	250.4827	0.03	250.2867	−0.05	250.4416	0.01
$\omega_1^1+\omega_2^1$	−134.1468	−134.1055	−0.03	−134.0375	−0.08	−134.0898	−0.04

Table 27 Strain components for [45 30 90 0]$_S$ laminate

	Applied load $N_{12} = 1$ N/m, $N_{21} = 1$ N/m						
		Paraboloid		Cylinder		Hyperboloid	
	$10^{-9} \cdot$ P.A.	$10^{-9} \cdot$ P.E.	Error %	$10^{-9} \cdot$ P.E.	Error %	$10^{-9} \cdot$ P.E.	Error %
e_1^0	−1.0079	−0.7595	−24.65	−0.7595	−24.64	−0.7596	−24.63
e_2^0	−0.6522	0.0101	−101.55	0.0103	−101.59	0.0098	−101.5
$\omega_1^0 + \omega_2^0$	4.6422	15.0629	224.48	15.0727	224.69	15.0727	224.69
e_1^1	0	4.4698	N/A	9.3903	N/A	11.1622	N/A
e_2^1	0	−5.8539	N/A	−9.0599	N/A	−9.2426	N/A
$\omega_1^1 + \omega_2^1$	0	−134.0898	N/A	−70.5098	N/A	3.3273	N/A

Table 28 Strain components for [45 30 90 0]$_S$ laminate

	Applied load $M_{12} = 1$ N and $M_{21} = R_2/R_1$ N								
	Paraboloid			Cylinder			Hyperboloid		
	$M_{21} = R_2/R_1 = 1.5$ N			$M_{21} = R_2/R_1 = 0$ N			$M_{21} = R_2/R_1 = -1$ N		
	P.A.	P.E.	Error %	P.A.	P.E.	Error %	P.A.	P.E.	Error %
e_1^0	0	−3.0711	N/A	0	−2.0371	N/A	0	−2.0275	N/A
e_2^0	0	−8.1779	N/A	0	−5.455	N/A	0	−5.4364	N/A
$\omega_1^0 + \omega_2^0$	0	−128.7234	N/A	0	−85.9029	N/A	0	−85.9085	N/A
e_1^1	N/A	−350.0595	N/A	N/A	−281.5233	N/A	N/A	−235.2312	N/A
e_2^1	N/A	−118.5717	N/A	N/A	53.8131	N/A	N/A	168.631	N/A
$\omega_1^1 + \omega_2^1$	N/A	2235.7513	N/A	N/A	947.4728	N/A	N/A	87.1956	N/A

symmetry of the stress resultants implies $M_{12} = M_{21}$. However, Eq. (13) is more appropriate and if $N_{12} = N_{21} = 0$ and $M_{12} = 1$, then $M_{21} = R_2/R_1$.

It is noted that due to Eq. (13), the stiffness matrix of Eq. (20) is singular and cannot be inverted as is. This problem is easily overcome, because by using Eq. (13) and by noting that $\tilde{\omega}_1^0$ is equal to $\tilde{\omega}_2^0$, due to Eq. (40), it is possible to reduce the 10 by 10 singular stiffness matrix to a 9 by 9 for which the determinant is nonzero.

VI. Conclusions

General equations of multilayered anisotropic shells were developed by including the effects of shear deformation, initial curvature, and geometrically nonlinear deformation effects. A novel expression for the stiffness matrix has been presented in which the relationship between the shell shape and the stiffness coefficients has been made explicit.

It is noted that the linear part of the developed model is in good agreement with results from [4]; the model has been further extended to include the effects of geometrically nonlinear deformations and to take into account and solve the most common theoretical inconsistencies of previous formulations. Precisely, retaining the coefficient $1 + \zeta/R_i$ in the definition of stress resultants has made it possible to satisfy the equation of drilling equilibrium. Also, because it is based on the work by Reddy [9,10], the present model does not give nonphysical strain and stress resultants due to rigid-body motion.

The role of geometry (initial curvatures) as a source of anisotropy has been analyzed. It has been shown that the effect of curvature significantly affects the bending-stretching matrix and that its magnitude depends on the sign of the Gaussian curvature and on the degree of symmetry of lamination. Generally, each element of the stiffness matrix partially depends on the thickness/local radius of curvature ratio and on the Gaussian curvature.

The stiffness coefficients presented herein differ from those obtained with the plate approximation, giving errors up to 5–8% for values of thickness-to-radius ratios of the order of 0.1. It is shown that neglecting curvature effects may lead to variations of the strain components from a few to several dozens of percentage points. It is noted that such a difference may significantly affect buckling and postbuckling phenomena.

Acknowledgments

The authors thank the funding of Airbus United Kingdom and South West Regional Development Agency through a Great Western Research grant.

References

[1] Weaver, P. M., "On Beneficial Anisotropic Effects in Composite Structures," 43rd AIAA/ASME/ASCE/AHS/ASC Structures, Structural Dynamics, and Materials Conference, Denver, CO, AIAA Paper 2002-1582, Apr. 2002.

[2] Qatu, M. S., "Recent Research Advances in the Dynamic Behavior of Shells: 1989–2000, Part 1: Laminated Composite Shells," *Applied Mechanics Reviews*, Vol. 55, No. 4, 2002, pp. 325–350. doi:10.1115/1.1483079

[3] Toorani, M. H., and Lakis, A. A., "General Equations of Anisotropic Plates and Shells Including Transverse Shear Deformation, Rotary Inertia and Initial Curvature Effects," *Journal of Sound and Vibration*, Vol. 237, No. 4, 2000, pp. 561–615. doi:10.1006/jsvi.2000.3073

[4] Qatu, M. S., "Accurate Equations for Laminated Composite Deep Thick Shells," *International Journal of Solids and Structures*, Vol. 36, No. 19, 1999, pp. 2917–2941. doi:10.1016/S0020-7683(98)00134-6

[5] Qatu, M. S., "Reply to Comments by Soldatos, K. P. on the 'Accurate Equations for Laminated Composite Deep Thick Shells,'" *International Journal of Solids and Structures*, Vol. 37, No. 29, 2000, pp. 4037–4038. doi:10.1016/S0020-7683(99)00234-6

[6] Gol'denveizer, A. L., *Theory of Elastic Thin Shells*, Pergamon, London, 1961.

[7] Voyiadjis, G. Z., and Shi, G., "A Refined Two-Dimensional Theory for Thick Cylindrical Shells," *International Journal of Solids and Structures*, Vol. 27, No. 3, 1991, pp. 261–282. doi:10.1016/0020-7683(91)90082-Q

[8] Voyiadjis, G. Z., and Woelke, P., "A Refined Theory for Thick Spherical Shells," *International Journal of Solids and Structures*, Vol. 41, No. 14, 2004, pp. 3747–3769. doi:10.1016/j.ijsolstr.2004.02.022

[9] Reddy, J. N., "Exact Solutions of Moderately Thick Laminated Shells," *Journal of Engineering Mechanics*, Vol. 110, No. 5, 1984, pp. 794–809.

[10] Reddy, J. N., *Mechanics of Laminated Composite Plates and Shells: Theory and Analysis*, 2nd ed., CRC Press, Boca Raton, FL, 2004.

[11] Novozhilov, V. V., *Foundation of the Nonlinear Theory of Elasticity*,

Dover, Mineola, NY, 1999.
[12] Novozhilov, V. V., *The Theory of Thin Shells*, Wolters-Noordhoff, Groningen, The Netherlands, 1959.
[13] Sanders, J. L., Jr., "An Improved First Approximation Theory for Thin Shells," NASA TR-R24, 1959.
[14] Budiansky, B., and Sanders, J. L., Jr., "On the 'Best' First-Order Linear Shell Theory," *Progress in Applied Mechanics*, Vol. 20, Springer, New York, 1963, pp. 129–140.
[15] Sanders, J. L., Jr., "Nonlinear Theories for Thin Shells," *Quarterly of Applied Mathematics*, Vol. 21, No. 1, 1963, pp. 21–36.
[16] Gray, A., Abbena, E., and Salamon, S., *Modern Differential Geometry of Curves and Surfaces with Mathematica*, 3rd ed., Chapman & Hall/ CRC, Boca Raton, FL, 2006.
[17] Budiansky, B., "Notes on Nonlinear Shell Theory," *Journal of Applied Mechanics*, Vol. 35, No. 2, 1968, pp. 393–401.
[18] Koiter, W. T., "On Foundations of Linear Theory of Thin Elastic Shells, 1," *Proceedings of the Koninklijke Nederlandse Akademie van Wetenschappen Series B, Physical Sciences*, Vol. 73, No. 3, 1970, pp. 169– 195.
[19] Koiter, W. T., *A Consistent First Approximation in the General Theory of Thin Elastic Shells. Part 1: Foundations and Linear Theory*, Lab. voor Toegepaste Mechanica der Technische Hogeschool, Delft, The Netherlands, 1959.
[20] Koiter, W. T., "Foundations and Basic Equations of Shell Theory," *Proceedings of IUTAM, Second Symposium Theory on Theory of Thin Shells*, Springer, New York, 1967, pp. 93–105.
[21] Niordson, F. I., *A Consistent Refined Shell Theory*, Dept. of Solid Mechanics, Technical Univ. of Denmark, Lyngby, Denmark, 1976.
[22] Grigorenko, Ya. M., "Approaches to the Numerical Solution of Linear and Nonlinear Problems in Shell Theory in Classical and Refined Formulations," *International Applied Mechanics*, Vol. 32, No. 6, 1996, pp. 409–442.
[23] Calladine, C. R., *Theory of Shell Structures*, Cambridge Univ. Press, Cambridge, England, U.K., 1983.
[24] Hoskin, B. C., and Baker, A. A., *Composite Materials for Aircraft Structures*, AIAA, New York, 1986.
[25] Pao, Y. C., "Simple Bending Analysis of Laminated Plates by Large-Deflection Theory," *Journal of Composite Materials*, Vol. 4, No. 3, 1970, pp. 380–389.
doi:10.1177/002199837000400309
[26] Donnell, L. H., *Beams, Plates and Shells*, McGraw–Hill, New York, 1976.
[27] Niordson, F. I., *Shell Theory*, North-Holland Series in Applied Mathematics and Mechanics, Vol. 29, North-Holland, Amsterdam, 1985.
[28] Palazotto, A. N., and Dennis, S. T., *Nonlinear Analysis of Shell Structures*, AIAA Education Series, AIAA, Washington, D.C., 1992.
[29] Ogden, R. W., *Non-Linear Elastic Deformations*, Dover, Mineola, NY, 1984.
[30] Pogorelov, A. V., *Bendings of Surfaces and Stability of Shells*, Translations of Mathematical Monographs, Vol. 72, American Mathematical Society, Providence, RI, 1988.
[31] Chia, C.-Y., *Nonlinear Analysis of Plate*, McGraw–Hill, New York, 1980.
[32] Cox, H. L., *The Buckling of Plates and Shells*, Pergamon, Oxford, 1963.
[33] Widera, O. E., "An Asymptotic Theory for the Moderately Large Deflections of Anisotropic Plates," *Journal of Engineering Mathematics*, Vol. 3, No. 3, 1969, pp. 239–244.
[34] Librescu, L., and Schmidt, R., "Refined Theories of Elastic Anisotropic Shells Accounting for Small Strains and Moderate Rotations," *International Journal of Non-Linear Mechanics*, Vol. 23, No. 3, 1988, pp. 217–229.
[35] Pai, P. F., and Nayfeh, A. H., "A Nonlinear Composite Plate Theory," *Nonlinear Dynamics*, Vol. 3, No. 6, 1992, pp. 431–463.
[36] Pai, P. F., and Nayfeh, A. H., "A Unified Nonlinear Formulation for Plate and Shell Theories," *Nonlinear Dynamics*, Vol. 6, No. 4, 1994, pp. 459–500.
[37] Yu, W., and Hodges, D. H., "A Geometrically Nonlinear Shear Deformation Theory for Composite Shells," *Journal of Applied Mechanics*, Vol. 71, No. 1, 2004, pp. 1–9.
[38] Cho, M., and Parmerter, R. R., "Efficient Higher-Order Composite Plate Theory for General Lamination Configurations," *AIAA Journal*, Vol. 31, No. 7, 1993, pp. 1299–1306.
doi:10.2514/3.11767
[39] Chia, C.-Y., and Chia, D. S., "Effect of Transverse Shear on Finite Deformation of Generally Laminated Shallow Shell with Double Curvature," *Acta Mechanica Solida Sinica*, Vol. 9, No. 1, 1996, pp. 27–41.
[40] Chia, C.-Y., "Nonlinear Analysis of Doubly Curved Symmetrically Laminated Shallow Shells with Rectangular Planform," *Archive of Applied Mechanics (Ingenieur Archiv)*, Vol. 58, No. 4, 1988, pp. 252–264.

A. Palazotto
Associate Editor